Inorganic Chemistry

ARTICLE

pubs.acs.org/IC

Syntheses and Characterization of Copper(II) Carboxylate Dimers Formed from Enantiopure Ligands Containing a Strong $\pi\cdots\pi$ Stacking Synthon: Enantioselective Single-Crystal to Single-Crystal Gas/Solid-Mediated Transformations

Daniel L. Reger,* Jacob J. Horger, Agota Debreczeni, and Mark D. Smith

Department of Chemistry and Biochemistry, University of South Carolina, Columbia, South Carolina 29208, United States

Supporting Information

ABSTRACT: Tri- and tetrafunctional enantiopure ligands have been prepared from 1,8-naphthalic anhydride and the amino acids L-alanine, D-phenylglycine, and L-asparagine to produce (*S*)-2-(1,8-naphthalimido)propanoic acid (HL_{ala}), (*R*)-2-(1,8-naphthalimido)-2-phenylacetic acid (HL_{phg}), and (*S*)-4-amino-2-(1,8 naphthalimido)-4-oxobutanoic acid (HL_{asn}), respectively. Reactions of L_{ala}^- with copper(II) acetate under a variety of solvent conditions has led to the formation and characterization by X-ray crystallography of three similar copper(II) paddlewheel complexes with different axial ligands, $[Cu_2(L_{ala})_4(THF)_2]$ (**1**), $[Cu_2(L_{ala})_4(HL_{ala})]$ (**2**), and $[Cu_2(L_{ala})_4(py)(THF)]$ (**3**). A similar reaction using THF and L_{phg}^- leads to the formation of $[Cu_2(L_{phg})_4(THF)_2]$ (**4**). With the exception of a disordered component in the structure of **4**, the naphthalimide groups in all of these compounds are arranged on the same side of the square, central paddlewheel unit, forming what is known as the chiral crown configuration. A variety of $\pi\cdots\pi$ stacking interactions of the 1,8-naphthalimide groups organize all of these complexes into supramolecular structures. The addition of the amide group functionality in the L_{asn}^- ligand leads to the formation of tetrameric $[Cu_4(L_{asn})_8(py)(MeOH)]$ (**5**), where reciprocal axial coordination of one of the amide carbonyl oxygen atoms between two dimers leads to the tetramer. Extensive supramolecular interactions in **5**, mainly the $\pi\cdots\pi$ stacking interactions of the 1,8-naphthalimide supramolecular synthon, support an open three-dimensional structure containing large pores filled with solvent. When crystals of $[Cu_4(L_{asn})_8(py)(MeOH)]$ are exposed to (*S*)-ethyl lactate vapor, the coordinated methanol molecule is replaced by (*S*)-ethyl lactate, bonding to the copper ion through the carbonyl oxygen, yielding $[Cu_4(L_{asn})_8(py)((S)\text{-ethyl lactate})]$ (**6**) without a loss of crystallinity. With the exception of the replacement of the one axial ligand, the molecular structures of **5** and **6** are very similar. In a similar experiment of **5** with vapors of (*R*)-ethyl lactate, again a change occurs without a loss of crystallinity, but in this case the (*R*)-ethyl lactate displaces only slightly more than half of the axial methanol molecules forming $[Cu_4(L_{asn})_8(py)\{((R)\text{-ethyl lactate})_{0.58}(MeOH)_{0.42}\}]$ (**7**). Importantly, in **7**, the (*R*)-ethyl lactate coordinates through the hydroxyl group. When crystals of $[Cu_4(L_{asn})_8(py)(MeOH)]$ are exposed to vapors of racemic ethyl lactate, the coordinated methanol molecule is displaced without a loss of crystallinity *exclusively* by (*S*)-ethyl lactate, yielding a new form of the tetramer $[Cu_4(L_{asn})_8(py)((S)\text{-ethyl lactate})]$, in which the ethyl lactate in the pocket bonds to the copper(II) ion through the carbonyl oxygen as with **6**. Exposure of $[Cu_4(L_{asn})_8(py)\{((R)\text{-ethyl lactate})_{0.58}(MeOH)_{0.42}\}]$ to *racemic* ethyl lactate yields a third form of $[Cu_4(L_{asn})_8(py)((S)\text{-ethyl lactate})]$, where the three forms of $[Cu_4(L_{asn})_8(py)((S)\text{-ethyl lactate})]$ have differences in the number of ordered (*S*)-ethyl lactate molecules located in the interstitial sites. These results demonstrate enantioselective bonding to a metal center in the chiral pocket of both **5** and **7** during single-crystal to single-crystal gas/solid-mediated exchange reactions.

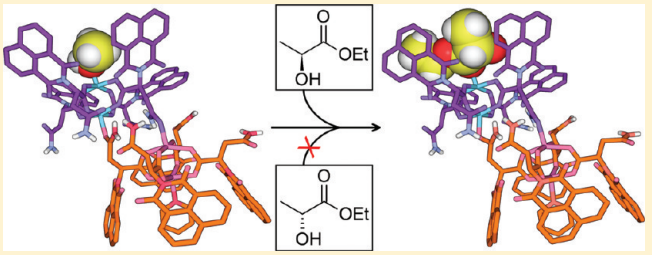

INTRODUCTION

Investigations of framework complexes comprised of metal centers linked by organic spacers are important in many fields of chemistry and materials science because of potential applications as catalysts,[1] molecular sensors,[2] and molecular sieves[3] and in the design of materials with interesting physical properties. These types of complexes can have a range of rigidity depending on the makeup of the organic linkers and the types of bonding interactions, both covalent and noncovalent, from which the structures are built.

One important structural type that has been extensively studied is formed by rigid metallic building blocks, referred to as secondary building units (SBUs), organized into ordered structures by robust organic linkers, compounds generally referred to as metal-organic frameworks (MOFs).[4,5] Multidentate linkers such as carboxylates are used to prepare the SBU in the formation of these rigid MOFs; these ligands have the added

Received: June 9, 2011
Published: September 15, 2011

Scheme 1. Bifunctional Carboxylate Ligands Containing the 1,8-Naphthalimide Group

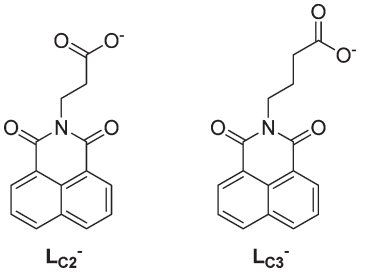

Scheme 2. Enantiopure Trifunctional (L_{ala}^-, L_{phg}^-) and Tetrafunctional (L_{asn}^-) Ligands Containing the 1,8-Naphthalimide Group

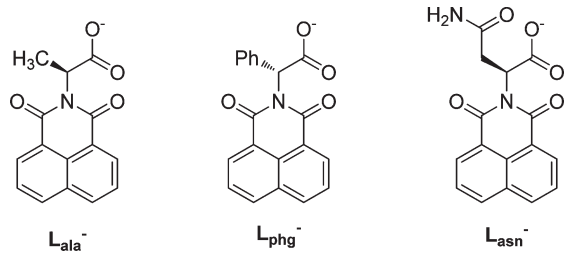

advantage of producing neutral metal clusters that do not contain counterions that would fill potential open spaces in the structures.

Monodentate ligand to metal coordination linkages (using mostly rigid pyridine-based ligands) are also widely used to support the formation of these types of structures. Frameworks built partially or completely by these interactions can be viewed as somewhat different from MOFs, as the stability of the network is reduced such that the framework is more likely to collapse upon the removal of solvent molecules occupying spaces in the structure.[6]

Much less rigid but still highly organized structures can be built with noncovalent supramolecular interactions. Hydrogen bonding is the most widely used organizational synthon in these materials, which has the potential advantage (and disadvantage in some cases) of creating more flexible materials that are more "elastic" in their properties.[7] Other types of noncovalent interactions, most notably $\pi\cdots\pi$ stacking of aromatic groups, have been used in the construction of flexible materials.[8]

We are attempting to construct framework complexes that combine the rigidity of the central SBU core with the supramolecular organization provided by *unusually strong* $\pi\cdots\pi$ stacking interactions. Given that the established order of stability of $\pi\cdots\pi$ interactions is π-deficient $-$ π-deficient > π-deficient $-$ π-rich > π-rich $-$ π-rich,[8a] we have recently incorporated the π-deficient, extended aromatic 1,8-naphthalimide group as an important noncovalent bonding synthon into multifunctional poly(pyrazolyl)methane ligands. We have shown that metal complexes of these ligands are organized into highly ordered structures by this functional group using strong noncovalent interactions, interactions that persist in solution.[9] An additional important advantage of this supramolecular synthon is synthetic convenience—the 1,8-naphthalimide group can easily be introduced into different types of ligand systems.

More recently, we have prepared bifunctional carboxylate ligands containing this supramolecular synthon (Scheme 1).[10] Using these ligands to prepare metal complexes with the well-known copper(II) carboxylate dimers (paddlewheels) as the SBU produced interesting three-dimensional structures. The copper(II) carboxylate system was chosen for its "square" paddlewheel architecture and its ability to strongly coordinate to axial ligands.[11]

We report here that the introduction into these types of ligands of an enantiopure chiral center from an amino acid, Scheme 2, leads to the syntheses of copper(II) carboxylate dimers and asparagine tetramers that have interesting molecular and supramolecular structures. We anticipated the preparation of homochiral complexes, with unique structures organized by the square-shaped SBU and the 1,8-naphthalimide supramolecular synthon, that have unusual properties.[12−15] Of particular interest in the results reported here are the tetrameric complexes prepared from the asparagine ligand where the open supramolecular structures combined with the chirality of the ligands lead to the observation of enantioselective exchange of axial ligands during single-crystal to single-crystal gas/solid-mediated transformations. Chiral rhodium(II) complexes of enantiopure carboxylate ligands related to those reported here (mainly phthalimide derivatives) have been used previously as catalysts to support asymmetric cyclopropanation and C−H insertion reactions,[16,17] and only recently have a number of these complexes been structurally characterized, including one example of a copper(II) dimer.[16g,17b,18] We have previously communicated some of these results.[19]

EXPERIMENTAL SECTION

General Considerations. Unless otherwise specified, all operations were carried out with no special precautions to exclude air or moisture. All solvents and reagents were used as purchased. (*R*)-ethyl lactate was produced by transesterification of commercially available (*R*)-methyl lactate with ethanol and purified by kugelrohr distillation; enantiopurity was verified via ^{1}H NMR by the addition of a small amount of the chiral shift reagent ErFOD. Analytical figures for the metal complexes were carried out on crystals dried to a constant weight.

General Procedure for Preparation of Ligands. To a stirred solution of the desired amino acid (22 mmol) in water (25 mL) was added solid potassium hydroxide (1.12 g, 20 mmol). This solution was allowed to stir for 20 min, and 1,8-naphthalic anhydride (3.96 g, 20 mmol) and ethanol (75 mL) were added. The solution was heated at reflux for 6−8 h, during which time the cream-colored suspension of 1,8-naphthalic anhydride dissolved. The heat was removed, and a solution of 1 M aqueous HCl (20 mL, 20 mmol) was added. The stirring was stopped, and the reaction mixture was allowed to stand undisturbed overnight. The solid product that formed was filtered and washed with 4 × 50 mL portions of water followed by 50 mL of ice-cold anhydrous ethanol. The solid was dried under vacuum conditions overnight to afford analytically pure 1,8-naphthalimide-substituted amino acids.

*(S)-2-(1,8-Naphthalimido)propanoic Acid (H**L**$_{ala}$).* Prepared as above, starting from L-alanine (1.96 g, 22 mmol). Yield: 4.59 g (85%). ^{1}H NMR ($CDCl_3$): δ 8.62 (d, J = 7.3 Hz, 2 H, 2-*nphth*), 8.24 (d, J = 8.2 Hz, 2 H, 4-*nphth*), 7.77 (t, J = 7.6 Hz, 2 H, 3-*nphth*), 5.84 (q, J = 7.0 Hz, 1 H, α-*CH*), 1.71 (d, J = 7.1 Hz, 3 H, β-CH_3). Anal. Calcd for $C_{15}H_{11}NO_4$: C, 66.91; H, 4.12; N, 5.20. Found: C, 66.85; H, 3.91; N, 4.94.

*(R)-2-(1,8-Naphthalimido)-2-phenylacetic Acid (H**L**$_{phg}$).* Prepared as above, starting from D-phenylglycine (3.33 g, 22 mmol). Yield: 5.04 g (76%). ^{1}H NMR ($CDCl_3$): δ 8.97 (dd, J = 7.4, 0.9 Hz, 2 H, 2-*nphth*), 8.56 (dd, J = 7.9, 0.3 Hz, 2 H, 4-*nphth*), 8.10 (m, 4 H, 2,5-*Ph*, 3-*nphth*), 7.67 (m, 4 H, 3,4,5-*Ph*, α-C*H*). Anal. Calcd for $C_{20}H_{13}NO_4$: C, 72.50 H, 3.95; N, 4.23. Found: C, 72.63; H, 3.81; N, 3.48.

*(S)-4-Amino-2-(1,8-naphthalimido)-4-oxobutanoic Acid (H**L**$_{asn}$).* Prepared as above, starting from L-asparagine (2.91 g, 22 mmol). Yield: 4.83 g (75%). Due to the extremely low solubility of this compound in organic solvents, the NMR spectrum was measured as the potassium salt of the ligand. ^{1}H NMR (CD_3OD): δ 7.02 (d, J = 7.3 Hz, 2 H, 2-*nphth*), 6.80 (d, J = 8.5 Hz, 2 H, 4-*nphth*), 6.26 (t, J = 7.3 Hz, 2 H, 3-*nphth*), 4.44 (dd, J = 5.5, 8.8 Hz, 1 H, α-C*H*), 1.84, 1.45 (m, 2 H, β-CH_2). Anal. Calcd for $C_{16}H_{12}N_2O_5$: C, 61.54; H, 3.87; N, 8.97. Found: C, 61.29; H, 3.82; N, 8.79.

Preparation of Paddlewheel Complexes. *[Cu$_2$(**L**$_{ala}$)$_4$(THF)$_2$] (**1**).* To a powdered sample of H**L**$_{ala}$ (1.07 g, 4.0 mmol) suspended in water (40 mL) was added a solution of 1 M KOH in methanol (4 mL, 4.0 mmol). This solution was stirred until the suspension had completely cleared (ca. 5 min). To this solution was added a solution of copper(II) acetate (400 mg, 1.0 mmol) in water (40 mL). A purple precipitate formed immediately. This mixture was stirred for 2 h, and the purple precipitate was isolated by filtration and washed twice with each water, absolute ethanol, and diethyl ether. After drying under vacuum conditions, this powder was dissolved in a minimal amount of 1:1 THF/CH_2Cl_2. An equal volume of hexane was added, and the solvents were removed via rotary evaporation to give the title compound (1.02 g, 76%) as a green powder. Single crystals were grown by layering hexane on top of a THF solution of the title compound (ca. 5 mg/mL) and allowing the solutions to rest undisturbed in a quiet location. Crystals suitable for X-ray analysis were obtained after 1−3 days. Anal. Calcd for $C_{68}H_{56}N_4O_{18}Cu_2$: C, 60.76; H, 4.20; N, 4.17. Found: C, 60.61; H, 4.07; N, 4.25.

*[Cu$_2$(**L**$_{ala}$)$_4$(H**L**$_{ala}$)] (**2**).* This compound was prepared by the same procedure as for [Cu$_2$(**L**$_{ala}$)$_4$(THF)$_2$], with the intermediate purple product being redissolved in a minimal amount of pure CH_2Cl_2 instead of a mixed CH_2Cl_2/THF system. Yield: 882 mg, 60%. Single crystals were grown by layering hexane on top of a CH_2Cl_2 solution of the title compound (ca. 5 mg/mL) and allowing the solutions to rest undisturbed in a quiet location.

*[Cu$_2$(**L**$_{ala}$)$_4$(py)(THF)] (**3**).* This compound was prepared by the same procedure as for [Cu$_2$(**L**$_{ala}$)$_4$(THF)$_2$], but with the addition of pyridine (0.2 mL) to the aqueous solution of copper acetate. Yield: 1.05 g, 78%. Single crystals were grown by layering hexane on top of a THF solution of the title compound (ca. 5 mg/mL) and allowing the solutions to rest undisturbed in a quiet location. Anal. Calcd for $C_{69}H_{53}N_5O_{17}Cu_2$: C, 61.33; H, 3.95; N, 5.18. Found: C, 61.17; H, 4.23; N, 4.96.

*[Cu$_2$(**L**$_{phg}$)$_4$(THF)$_2$] (**4**).* This compound was prepared by the same procedure as [Cu$_2$(**L**$_{ala}$)$_4$(THF)$_2$], starting with H**L**$_{phg}$ (1.33 g, 4.0 mmol). The title compound (1.29 g, 81%) was isolated as a green powder. Single crystals were grown by layering hexane on top of a THF solution of the title compound (ca. 5 mg/mL) and allowing the solutions to rest undisturbed in a quiet location. Anal. Calcd for $C_{88}H_{64}N_4O_{18}Cu_2$: C, 66.37; H, 4.05; N, 3.52. Found: C, 64.24; H, 4.01; N, 3.26.

*[Cu$_4$(**L**$_{asn}$)$_8$(py)(MeOH)] (**5**).* This compound was prepared by the same procedure as [Cu$_2$(**L**$_{ala}$)$_4$(THF)$_2$], except a small amount of pyridine was added to the copper(II) acetate solution, starting with H**L**$_{asn}$ (1.25 g, 4.0 mmol), with the intermediate purple product being redissolved in approximately 400 mL of 1:9 MeOH/CH_2Cl_2 instead of a mixed CH_2Cl_2/THF system. Yield: 1.26 g, 88%. Single crystals were grown by layering diethyl ether on top of a 1:9 MeOH/CH_2Cl_2 solution of the title compound (ca. 5 mg/mL) and allowing the solutions to rest undisturbed in a quiet location. Crystals suitable for X-ray analysis were obtained after 4−7 days. Anal. Calcd for $C_{134}H_{97}N_{17}O_{41}Cu_4$: C, 56.36; H, 3.42; N, 8.34. Found: C, 56.53; H, 3.58; N, 8.12.

Scheme 3. General Synthesis of Enantiopure 1,8-Naphthalimide Ligands from Amino Acids

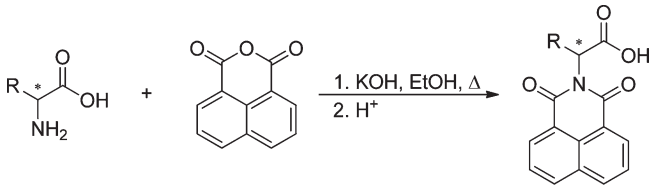

R = CH_3 (H**L**$_{ala}$), Ph (H**L**$_{phg}$), CH_2CONH_2 (H**L**$_{asn}$)

Vapor-Phase Single-Crystal to Single-Crystal Ligand Exchange. For the vapor-phase single-crystal to single-crystal ligand exchange, the crystallization solvent was carefully removed from a test tube containing a freshly grown sample of [Cu$_4$(**L**$_{asn}$)$_8$(py)(MeOH)] (without disturbing the crystals adhered to the walls of the tube), and the crystals were washed with a small amount of a 10:9:1 diethyl ether/dichloromethane/methanol mixture. The crystals were briefly allowed to air-dry (~30−60 s), and a small test tube lined with filter paper containing ~1 mL of the desired ligand ((*S*)-ethyl lactate (*S*-EtLac), racemic ethyl lactate, or (*R*)-ethyl lactate (*R*-EtLac)) was carefully placed inside the larger test tube. The system was sealed with a rubber septum and allowed to sit undisturbed for approximately 48 h. Single crystals were selected from the tube for X-ray crystallographic analysis and, for the cases of (*S*)-ethyl lactate and racemic ethyl lactate, shown to be [Cu$_4$(**L**$_{asn}$)$_8$(py)(*S*-EtLac)]. Anal. Calcd for $C_{138}H_{103}N_{17}O_{43}Cu_4$: C, 56.35; H, 3.53; N, 8.09. Found: C, 56.12; H, 3.43; N, 8.09. For the cases of (*R*)-ethyl lactate, they were shown to be [Cu$_4$(**L**$_{asn}$)$_8$(py){(*R*-EtLac)$_{0.58}$(MeOH)$_{0.42}$}]

X-Ray Crystallographic Data Collection and Refinement. All X-ray intensity data were measured at 150(2) K using a Bruker SMART APEX diffractometer (Mo Kα radiation, λ = 0.71073 Å).[20] Raw area detector data frame reduction and corrections for absorption effects were performed with the SAINT+ and SADABS programs.[20] Final unit cell parameters were determined by least-squares refinement of large sets of reflections from each data set. Direct methods structure solution, difference Fourier calculations, and full-matrix least-squares refinement against F^2 were performed with SHELXTL.[21] X-ray crystallographic data are given in Table S1 (Supporting Information), and detailed explanations of the refinement procedures, including the use of SQUEEZE[22] in certain structures, are given in the Supporting Information.

RESULTS

Syntheses. The tri- and tetrafunctional ligands were synthesized from commercially available amino acids in one pot (Scheme 3). In the presence of ethanolic potassium hydroxide, the amino acids are heated at reflux with 1,8-naphthalic anhydride to give (after precipitation with acid) the protonated form of the chiral carboxylate ligand, H**L**$_{aminoacid}$. H**L**$_{ala}$ and similar ligands using other amino acid analogues have been previously prepared using the conditions of refluxing 1,8-naphthalic anhydride in DMSO, DMF, or pyridine.[23] These reactions in DMSO or DMF, in our hands, could not reliably ensure the retention of configuration of the chiral center. The reaction conditions described here both prevent racemization of the amino acid chiral center (even in the case of the base-sensitive D-phenylglycine) and eliminate the need for chromatographic purification.

Scheme 4. Preparation of Paddlewheel Compounds from Enantiopure Carboxylate Ligands

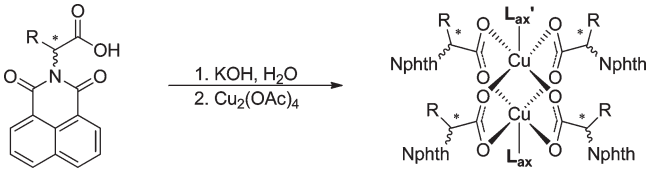

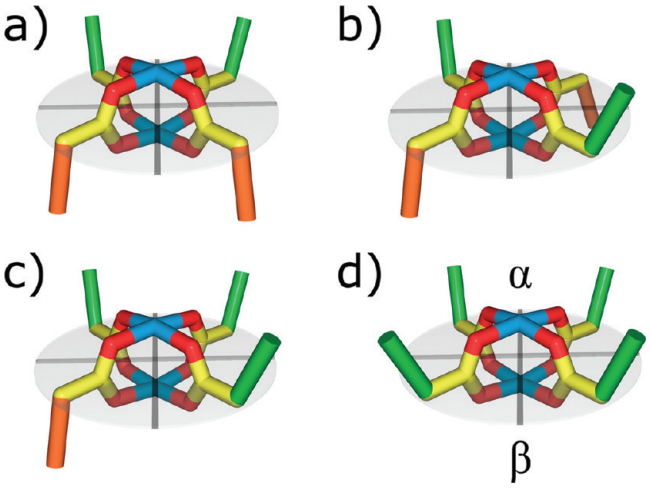

Figure 1. Four possible ligand configurations in chiral-ligand paddlewheel complexes.

To prepare the copper(II) paddlewheel complexes, the potassium salt of the ligand is generated in situ with KOH and allowed to react with copper(II) acetate (Scheme 4). If pyridine is desired as an axial ligand, it is added to the reaction mixture in slight excess. A water-insoluble purple intermediate product that has not been characterized precipitates from these reaction mixtures. Subsequent workup of this solid that precipitated in the reaction of the $\mathbf{L_{ala}}^-$ ligand with a THF/CH_2Cl_2 mixture followed by crystallization by layering a THF solution with hexane yields $[Cu_2(\mathbf{L_{ala}})_4(THF)_2]$ (**1**). A similar workup using pure CH_2Cl_2 in both steps yields $[Cu_2(\mathbf{L_{ala}})_4(H\mathbf{L_{ala}})]$ (**2**). In a $\mathbf{L_{ala}}^-$ reaction to which pyridine had been added, the workup as described above with a THF/CH_2Cl_2 mixture yields $[Cu_2(\mathbf{L_{ala}})_4(py)(THF)]$ (**3**). A similar reaction and workup that was used in **1** but using $\mathbf{L_{phg}}^-$ yields $[Cu_2(\mathbf{L_{phg}})_4(THF)_2]$ (**4**). Finally, a reaction similar to that discussed for **3** using $\mathbf{L_{asn}}^-$ and MeOH/CH_2Cl_2 instead of a mixed THF/CH_2Cl_2 system (for solubility reasons) in the workup and ether as the layering solvent yields $[Cu_4(\mathbf{L_{asn}})_8(py)(MeOH)]$ (**5**).

Structural Analysis. In all of the new complexes of the three ligands reported here, the core of each complex is the anticipated square, dimeric $Cu_2(O_2CR)_4$ "paddlewheel" SBU motif. Each carboxylate ligand surrounds the two copper atoms with μ^2-bonding placing the oxygen donor atoms in each of the four equatorial positions about the square pyramidal, five-coordinate copper ion sites. The fifth site is filled by the axial ligands. The Cu···Cu nonbonding distances are between 2.6 and 2.7 Å. Selected bond distances and angles are given in Tables S2 and S3 (Supporting Information), respectively.

As has been pointed out elsewhere,[24] although there are many conformations that complexes **1**−**4** can adopt, four possible arrangements of the substituents on the chiral ligands in relationship to the copper dimer core have mainly been considered. The large 1,8-naphthalimide groups can be arranged such that two are on each side of the square, central paddlewheel unit, with either a *cis* or *trans* orientation; three could be on one side, or all four could be on one side, Figure 1. Though the precise arrangement of the naphthalimide groups varies from complex to complex, all but part of one of the structures reported here show the naphthalimide groups all on one side (Figure 1d), adopting what has been termed in the rhodium dimer literature the "chiral crown" configuration.[16g,18a] Following that literature, the naphthalimide groups are oriented on the same side, forming a chiral, hydrophobic pocket defined as the α face, and the side chain "arms" of the ligand located at the chiral carbon are oriented on the opposite side defined as the β face.

Structure of $[Cu_2(\mathbf{L_{ala}})_4(THF)_2]$ (**1**). Figure 2 shows a numbered diagram for $[Cu_2(\mathbf{L_{ala}})_4(THF)_2]$ and the top view from the α face that illustrates the "chiral crown" configuration. On the α face, the naphthalimide groups are all canted in the same direction, a consequence of the enantiopure center in the ligands and the steric bulk of the naphthalimide groups. Four separate carboxylate ligands bridge the two copper(II) centers equatorially around the paddlewheel dimer. Molecules of THF coordinate to the copper ion sites at both the α and β faces. The chiral pocket formed by the naphthalimide groups is nearly symmetrical. Measuring the size of the pocket by taking the distance between the outside carbon (labeled C(10) in Figure 2) of naphthalimide groups *trans* across the pocket gives values of 13.9 Å and 13.8 Å.

Three copper(II) dimers of **1**, colored in Figure 3 as green, blue, and purple, are organized into trimeric units by $\pi\cdots\pi$ stacking interactions from two naphthalimide groups on each dimer. The interactions occur via the overlap of the outside face of one naphthalimide group in the chiral crown of one dimer with the inside face of a second naphthalimide group in the chiral crown on a second dimer. Each dimer makes one inside the pocket and one outside the pocket interaction using naphthalimide groups located on adjacent sides of the chiral pocket. These trimers are arranged so that the α faces of the bimetallic units are all oriented inward toward each other, while the β faces all point out. The $\pi\cdots\pi$ stacking interactions are strong; the planes of the two rings are separated vertically by 3.42 Å, and the rings are close to parallel with an interplanar angle of 5.7°. The rings also have substantial overlap, as measured by the "slippage" parameter χ, which is the third side of the right triangle formed with the average perpendicular distance between the rings and the line joining the central fused ring carbon atoms of the two rings. In this case, χ is 1.67 Å; we have shown previously that slippage in the range between 0.43 Å and 2.4 Å is indicative of a strong interaction.[10] The angle made by the two naphthalimide dipole vectors (running through the central ring carbon atoms, pointing toward the nitrogen), an additional parameter of interest in these systems, is 148°.

The π-stacked trimers pack close in the crystal into staggered zigzag layers in a repeating AB pattern; neighboring trimers do not have any substantial $\pi\cdots\pi$ stacking or other important noncovalent interactions with one another. Solvent-filled pores are formed by this AB repeating unit, which corresponds to the crystallographic *c* axis. The pores measure approximately 9.5 Å in diameter and contain ordered hexane and disordered THF

dx.doi.org/10.1021/ic201238n |*Inorg. Chem.* 2011, 50, 10225–10240

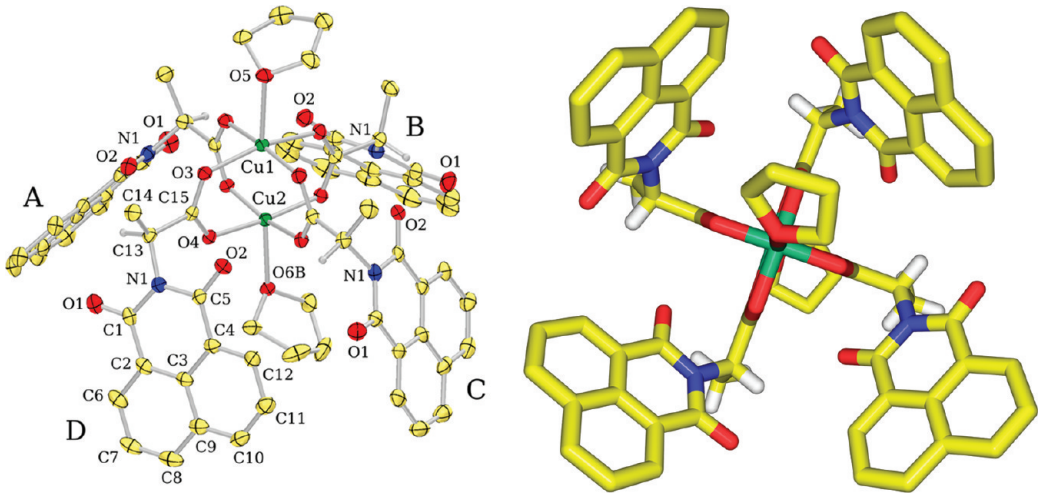

Figure 2. Left: Partially numbered diagram of $[Cu_2(L_{ala})_4(THF)_2]$ (**1**). Right: Top view of α-face chiral pocket.

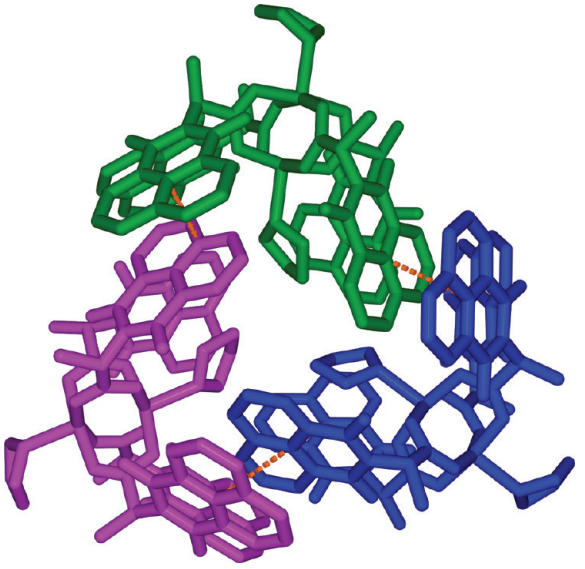

Figure 3. Naphthalimide $\pi\cdots\pi$ stacking interactions in $[Cu_2(L_{ala})_4(THF)_2]$ organizing the bimetallic units into a trimer.

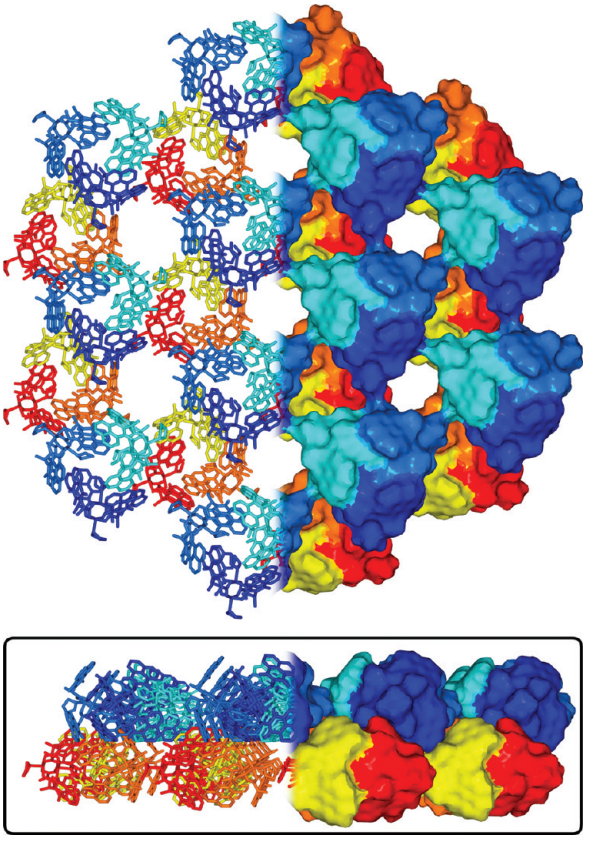

Figure 4. Top: Section of the overall structure of $[Cu_2(L_{ala})_4(THF)_2]$ showing the pores, viewed down the *c* axis. Layer A trimers are located above and are shown in shades of blue; layer B trimers are below in red and yellow. The molecular surface is shown on the right half of the image to more clearly indicate the pores. Bottom inset: edge-on view of the section on top showing the AB pattern in the stacking.

molecules. A view of the pores formed by packed trimers can be seen in Figure 4, where the two layers are color-coded. The molecular surface of each layer is shown on the right-hand side of the figure. Solvent molecules have been omitted for clarity.

Structure of $[Cu_2(L_{ala})_4(HL_{ala})]$ (**2**). When the same purple intermediate initially formed in the reaction of the L_{ala}^- ligand (used to grow crystals of **1**) is dissolved in the noncoordinating solvent dichloromethane so as to avoid adding potential axial ligands, $[Cu_2(L_{ala})_4(HL_{ala})]$ crystallizes. This dimer contains an additional protonated form of the ligand coordinated to the copper ion on the α face, as shown in Figure 5. Again, four carboxylate ligands bridge the equatorial sites of the paddlewheel. The carbonyl oxygen of the acid group of HL_{ala} is coordinated to the copper ion inside the α-face pocket with the OH of this group hydrogen-bonded to one of the equatorial carboxylate oxygen atoms. The chiral pocket measures 15.2 Å (B$\cdots$D) by 13.4 Å (A$\cdots$C).

The axial ligand for the copper ion located at the β face is a naphthalimide carbonyl oxygen from one of the four μ^2-carboxylate ligands on an adjacent dimer, forming a one-dimensional zigzag coordination polymer. Figure 6 shows six paddlewheel units of the polymer chain. Only a carbonyl group on one naphthalimide (from ligand A) in each dimer is involved in the chain formation; the other three μ^2-carboxylate ligands (B, C, and D) and the fifth, axial HL_{ala} (E), do *not* participate. We note that a coordination

dx.doi.org/10.1021/ic201238n |*Inorg. Chem.* 2011, 50, 10225–10240

polymer composed of dirhodium paddlewheel dimers derived from a similar enantiopure phthalimide-based ligand, linked by 1,4-dicyanobenzene, has been reported previously.[18a]

Two of the remaining equatorial naphthalimide groups (B, D) and the axial naphthalimide E participate in $\pi\cdots\pi$ stacking interactions. Four π-stacked dimers are shown in Figure 7—the ligands not participating in the π-stacking interaction have been omitted for clarity. Naphthalimide groups D and E from one dimer "clamp" a central equatorially coordinated naphthalimide (B′) from a neighboring dimer between them; similarly, naphthalimide B is itself clamped by naphthalimide groups from a different dimer. Both $\pi\cdots\pi$ stacking parts of the interaction are strong, with reasonable χ values between the central ring and the axial (χ_{BE} = 1.64 Å) and equatorial (χ_{BD} = 1.44 Å) arms of the "clamp." The vertical distances of 3.42 Å (B···D) and 3.48 Å (B···E) are also typical of strong interactions. All three planes are nearly parallel, with both B···E and B···D interplanar angles of 6°. This interaction forms one-dimensional zigzag chains, which run perpendicular to the direction of the coordination polymer.

The combination of the one-dimensional coordination polymer and the one-dimensional π-stacking interaction results in a fully three-dimensional structure. Each coordination polymer is π-stacked with four adjacent coordination polymers; Figure 8 is a cartoon representation of the framework showing these features. The inefficient packing of this structure leaves a considerable amount of space occupied by disordered dichloromethane

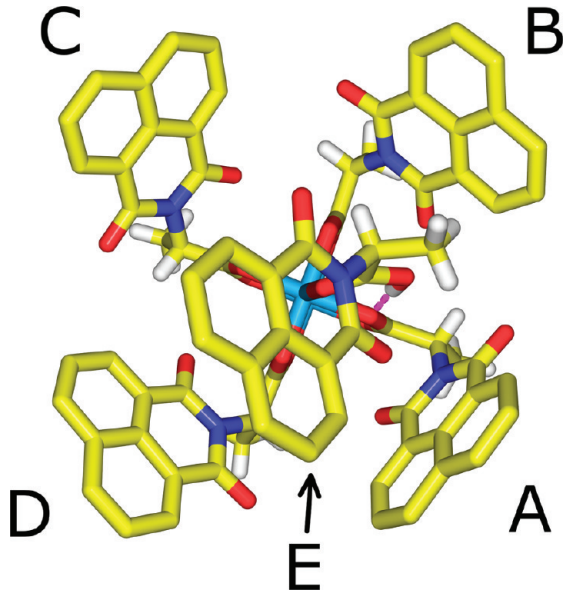

Figure 5. One $[Cu_2(\mathbf{L}_{ala})_4(\mathbf{HL}_{ala})]$ (**2**) unit, viewed toward the α face where the axial ligand is $\mathbf{HL}_{ala}$. The hydrogen-bonding interaction of this axial ligand is shown in magenta.

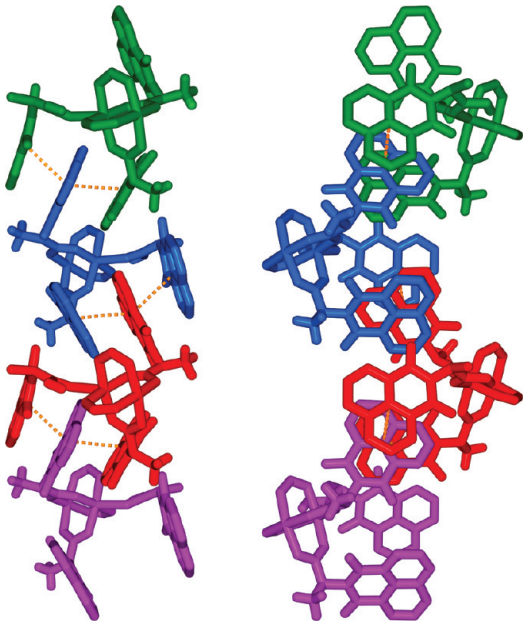

Figure 7. Naphthalimide−naphthalimide π stacking in $[Cu_2(\mathbf{L}_{ala})_4(\mathbf{HL}_{ala})]$. Separate dimeric units are shown in different colors. On the left, stacking interactions are indicated with orange dashed lines. The drawing on the right is a 90° rotation that shows the overlap of the naphthalimide rings.

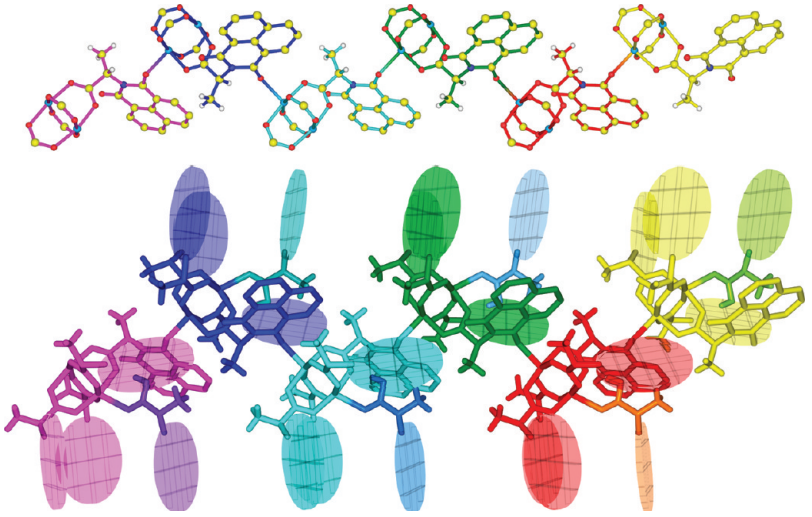

Figure 6. The polymeric chain formed by adjacent $[Cu_2(\mathbf{L}_{ala})_4(\mathbf{HL}_{ala})]$ dimers. Nonbridging naphthalimide groups are shown as transparent discs in the lower figure, colored to match the paddlewheel core to which they belong; the axial $\mathbf{HL}_{ala}$ units have a hue complementary to the rest of the paddlewheel.

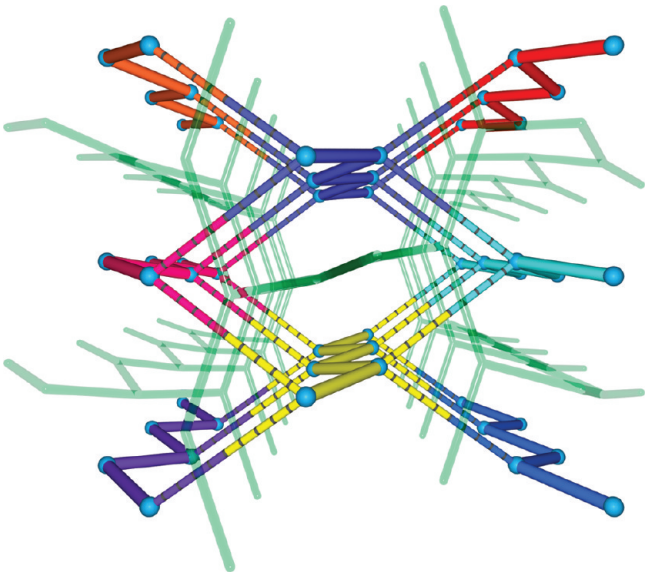

Figure 8. Simplified representation of the framework in $[Cu_2(\mathbf{L}_{ala})_4(\mathbf{HL}_{ala})]$. Thick colored cylinders indicate separate polymeric chains, where the SBU central dimeric unit is represented by a single blue sphere. Each polymer chain is $\pi\cdots\pi$ stacked with four other polymer chains, as indicated by the dashed cylinders. The network of dichloromethane molecules occupying the channels is indicated by transparent light green cylinders.

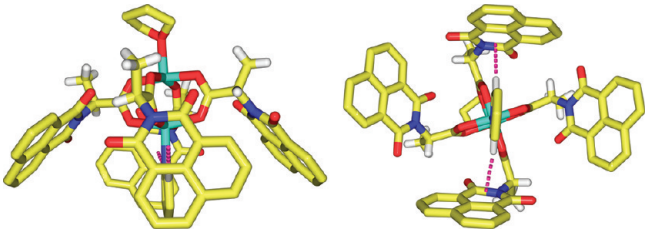

Figure 9. Two views of the dimer in $[Cu_2(\mathbf{L}_{ala})_4(py)(THF)]$ (**3**). Left: view from the side of the dimer. Right: view from the α-face pocket. The C−H$\cdots\pi$ interactions are shown in both as dashed magenta lines.

molecules. The dichloromethane molecules (light green lines) occupy three-dimensional channels that interpenetrate the network formed by the π-stacked coordination polymers.

Structure of $[Cu_2(\mathbf{L}_{ala})_4(py)(THF)]$ (**3**). When pyridine is present in the reaction mixture that formed the precursor for **1** and **2**, workup with a THF/CH_2Cl_2 mixture yields $[Cu_2(\mathbf{L}_{ala})_4(py)(THF)]$, a product that has two different ligands in the axial sites, one THF and one pyridine, as shown in Figure 9. The pyridine is bonded to the copper(II) ion inside the naphthalimide pocket of the α face with the THF molecule capping the β-face copper. The preference of pyridine for the chiral pocket appears to be driven by two C−H$\cdots\pi$ interactions from the 2 and 6 position hydrogens of the pyridine ring (shown as dashed magenta lines) with the nitrogen-containing ring of two of the naphthalimide groups (H$\cdots$centroid = 3.01, 3.02 Å, CH$\cdots$centroid = 179, 170°). These interactions cause asymmetry in the size of the naphthalimide pocket—the two naphthalimide groups that participate in the C−H$\cdots\pi$ interaction are 11.6 Å apart, as compared to 16.1 Å for the other two naphthalimide groups.

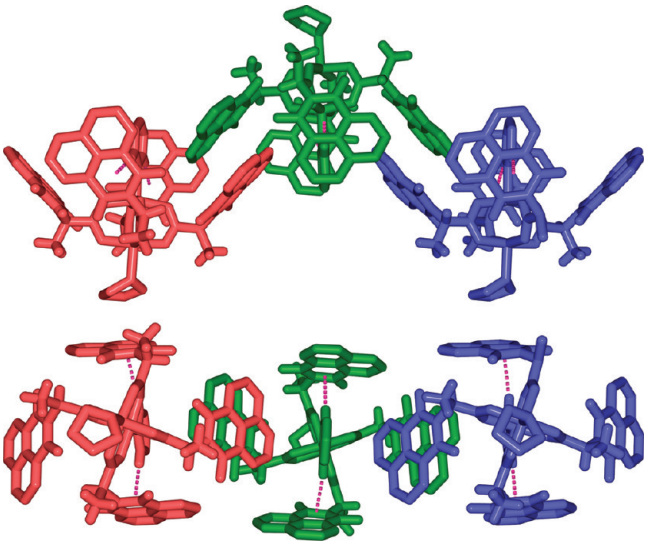

Figure 10. Three π-stacked units in a chain of **3**. The green-colored (central) dimer π-stacks with the red-colored (left) and blue-colored (right) dimers. Top: side view of the chain. Bottom: chain viewed from the α face of the green-colored dimer. The C−H$\cdots\pi$ interactions are shown as dashed magenta lines.

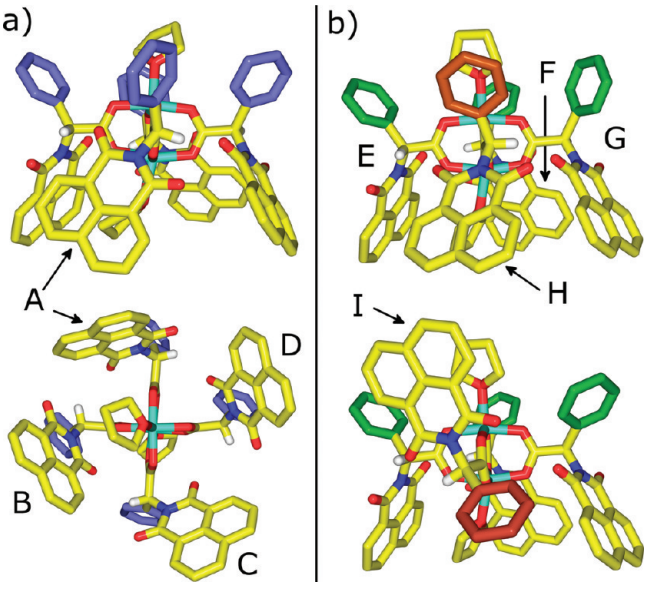

Figure 11. The two independent molecules in the structure of $[Cu_2(\mathbf{L}_{phg})_4(THF)_2]$ (**4**). (a) The ABCD dimer, viewed from the side (top) and from the α face (bottom). The phenyl rings are shown in blue. (b) A side view of the EFGH dimer (top) and the EFGI dimer (bottom). The phenyl rings associated with E, F, and G naphthalimide rings are shown in green, and the phenyl rings associated with H and I naphthalimide rings in red.

The two naphthalimide groups not participating in the C−H$\cdots\pi$ stacking interactions with pyridine $\pi\cdots\pi$ stack with naphthalimide groups on adjacent dimeric units with both rings interacting on the inside of the α-face pocket. These interactions are strong, being nearly parallel (2.8°) with a vertical separation of 3.39 Å, a χ value of 1.63 Å, and a naphthalimide−naphthalimide dipole vector angle of 119°. Three $\pi\cdots\pi$ stacked units (colored red, green, and blue) are shown in Figure 10; these interactions form one-dimensional chains where the dimers

dx.doi.org/10.1021/ic201238n |*Inorg. Chem.* 2011, 50, 10225–10240

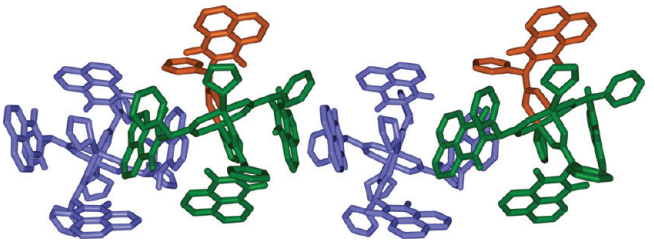

Figure 12. ABCD···EFG(H/I) $\pi\cdots\pi$ stacking interactions in the structure of **4**. Arms A, B, C, and D are shown in blue; arms E, F, and G in green; and arm I in red. Disorder component H is not shown.

alternate orientation (in the top figure, the α face goes up, down, up). There are no additional significant supramolecular interactions, yielding a one-dimensional structure.

*Structure of [Cu_2(**L_{phg}**)$_4$(THF)$_2$] (**4**).* The complex of the $\mathbf{L_{phg}}^-$ ligand, prepared analogously to $[Cu_2(\mathbf{L_{ala}})_4(THF)_2]$, crystallizes with two independent $[Cu_2(\mathbf{L_{phg}})_4(THF)_2]$ dimers in the unit cell, pictured in Figure 11. One dimer is fully ordered (with naphthalimide arms labeled A, B, C, and D) and displays the standard "chiral crown" conformation. It is important to note that the naphthalimide groups are canted in the opposite direction with respect to the other dimers discussed above—this change is due to the absolute configuration of the ligand (*R*), which was derived from a D-amino acid (D-phenylglycine) rather than an L-amino acid. The ABCD chiral pocket (like that observed in $[Cu_2(\mathbf{L_{ala}})_4(THF)_2]$) is almost symmetrical, measuring 13.4 Å × 13.2 Å. The other independent dimer has three ordered arms (E, F, and G), which are all on the same side (α-face), and a fourth arm, which exhibits a 2-fold rotational disorder over two equally occupied positions (H, α-oriented/I, β-oriented). The EFGH disorder component is almost isostructural with the ABCD dimer, with the chiral pocket formed by this component measuring 13.6 Å × 13.9 Å. The EFGI disorder component, unlike the rest of the complexes, has its naphthalimide groups arranged as Figure 1c, where only three of the naphthalimide groups are on one side. This disorder does not affect the conformation of the other naphthalimide groups but causes minor changes to the orientations of the phenyl side chains on arms E and G.

The ABCD dimer $\pi\cdots\pi$ stacks with the EFG(H/I) dimer via the naphthalimide groups of ligands B and D (Figure 12). One interaction occurs with naphthalimide groups using the inside faces of the chiral pockets (D···E) and one on the outside faces (B···G). As the $\pi\cdots\pi$ stacking of these dimers does not involve arm H/I, it is unaffected by the disorder. The values for these interactions are comparable to those seen for the other systems, with the "inside" $\pi\cdots\pi$ stacking having a vertical separation of 3.43 Å, a χ value of 1.91 Å, naphthalimide dipole vector angles oriented at 153°, and a very small interplanar angle (3°). The "outside" interactions have a similar vertical separation (3.42 Å) and are less slipped (χ = 1.01 Å). The naphthalimide—naphthalimide dipole angles are oriented at 138°, and the rings are almost coplanar (1° interplanar angle).

In addition to the ABCD···EFG(H/I) interaction, there are a number of other, weaker interactions involving the phenyl groups on the ligands (see the Supporting Information). These interactions, taken in combination with those outlined above, arrange the dimers into two-dimensional sheets, which have no significant additional supramolecular interactions. One sheet, as viewed from the β face of the ABCD paddlewheel, is shown in Figure 13. Only the EFGI disorder component is pictured.

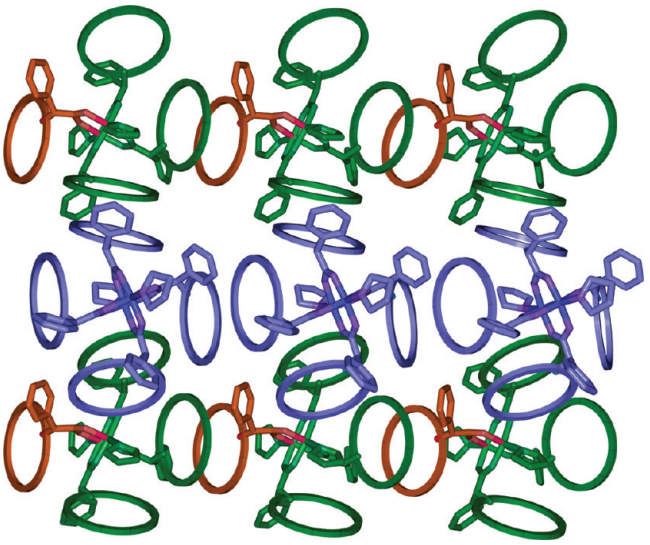

Figure 13. Axial view of one sheet formed by $[Cu_2(\mathbf{L_{phg}})_4(THF)_2]$ paddlewheels. Ligands E, F, and G are shown in green; ligand I is shown in red. The ABCD paddlewheel is colored blue. Naphthalimide groups are represented by colored hoops.

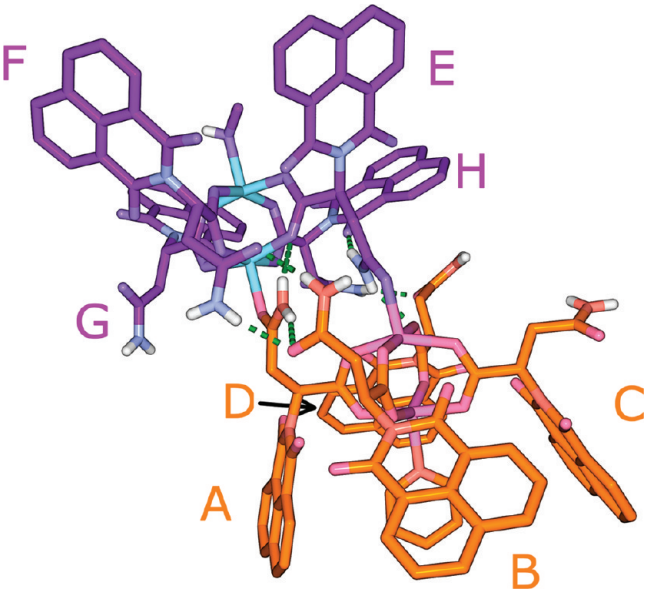

Figure 14. Drawing of the $[Cu_4(\mathbf{L_{asn}})_8(py)(MeOH)]$ (**5**) tetramer. The pyridine-coordinated dimeric subunit is shown in orange and the methanol-coordinated dimeric subunit in purple. Intramolecular hydrogen bonds are shown in green; hydrogen atoms attached to carbon have been omitted for clarity.

*Structure of [Cu_4(**L_{asn}**)$_8$(py)(MeOH)] (**5**).* The complex formed from the tetrafunctional $\mathbf{L_{asn}}^-$ ligand (the additional functionality being the amide substituent located on the side chain) retains the paddlewheel SBU central core, but two nonequivalent paddlewheel dimers are linked together via reciprocal axial coordination of one of the amide carbonyl oxygen atoms present in the ligand side chains of each dimer subunit to form tetramer $[Cu_4(\mathbf{L_{asn}})_8(py)(MeOH)]$. Figure 14 shows the structure of this tetramer. One dimeric subunit (shades of purple) has four carboxylate ligands (labeled E, F, G, and H) bridging the

Table 1. Hydrogen Bonding Parameters in $[Cu_4(L_{asn})_8(py)(MeOH)]$

D−H···A	D−H (Å)	H···A (Å)	D···A (Å)	<DHA (deg)
N(2A)−H(2A1)···O(5E)	0.88	2.35	3.09	141
N(2A)−H(2A2)···O(3B)	0.88	2.27	3.13	165
N(2B)−H(2B1)...O(3F)	0.88	2.06	2.93	170
N(2F)−H(2F1)···O(3B)	0.88	2.15	3.00	164
N(2E)−H(2E1)···O(5D)	0.88	2.05	2.81	144
N(2E)−H(2E2)···O(5E)	0.88	2.40	2.88	114
N(2E)−H(2E2)···O(1H)	0.88	2.04	2.83	148
N(2H)−H(2H2)···O(3D)	0.88	2.08	2.88	149

equatorial positions of the paddlewheel with a molecule of methanol (from the crystallization solvent) coordinated to the copper ion on the α-face pocket. The chiral pocket formed by these rings is more open than in the dimers described above, with a size of 16.5 Å (F···H) by 15.7 Å (E···G). The other dimeric subunit (shades of orange) also has four carboxylate ligands (labeled A, B, C, and D) present in its equatorial sites and has a pyridine coordinated to the copper ion in the α-face pocket. This axially coordinated pyridine shows the same pair of CH···π interactions as seen in $[Cu_2(L_{ala})_4(py)(THF)]$ (see Figure 9). The pocket is also similarly distorted by the pyridine, with the naphthalimide rings participating in the CH···π interaction (A and C) separated by 12.2 Å, compared to 15.2 Å for the noninteracting rings (B and D). The copper ions at the β face of both dimeric subunits are coordinated to an amide carbonyl oxygen from the other dimeric subunit through ligands A and E. These interactions are further supported by amide N−H···O (coordinated carboxylate) hydrogen bonds (E···D and A···E) from the axially coordinated amide NH_2 group. These bridging interactions bring the interdimer Cu···Cu distances down from over 10 Å in the dimeric structures described above to the shortest now being 6.56 Å. Additionally, there are a number of intramolecular hydrogen bonds between the "arms" of the ligands; the amide group from arm B hydrogen-bonds to amides from arms F and A, the amide from arm E to the naphthalimide group on arm H, and the arm D amide to the arm H amide. Parameters for these hydrogen-bonding interactions can be seen in Table 1.

These tetramers are organized into a complex supramolecular structure, mainly by π···π stacking interactions of the naphthalimide groups, where each dimeric subunit participates in different types of π-stacking motifs. These interactions link the tetramers into a fully three-dimensional structure. The pyridine-coordinated dimeric subunit of one tetramer π-stacks with the pyridine-coordinated subunit of two adjacent tetramers via the two naphthalimide groups *not* participating in the coordinated pyridine C−H···π interactions (B and D). This π···π stack is analogous to that seen with $[Cu_2(L_{ala})_4(py)(THF)]$, with both the interacting naphthalimide groups from adjacent units interacting on the inside of the α-face pocket (Figure 15). The metrics for the stacking interactions are also similar, with a χ value of 1.84 Å, a vertical separation of 3.51 Å, and a naphthalimide−naphthalimide dipole angle of 122°.

In the case of the methanol-coordinated subunit, all four of the naphthalimide groups participate in π···π stacking interactions with the MeOH-coordinated subunit of four adjacent tetramers. There are pairs of symmetrically equivalent interactions: two adjacent arms forming interactions on the outside of the pockets

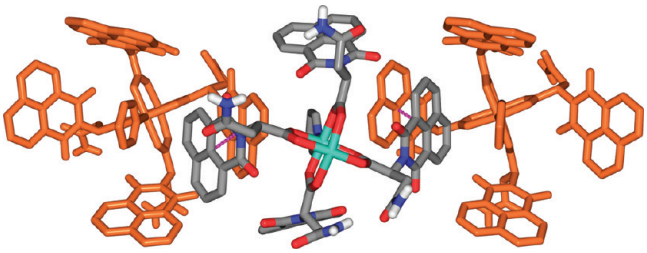

Figure 15. Naphthalimide π···π stacking interactions of the pyridine-coordinated subunit of $[Cu_4(L_{asn})_8(py)(MeOH)]$. The α face of the central dimeric subunit (viewed from the β face) π-stacks with the pyridine-coordinated subunits (viewed from the α faces) of adjacent subunits (shown in orange).

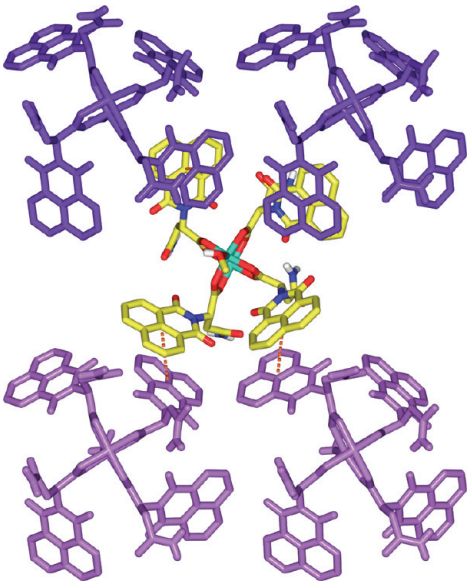

Figure 16. Naphthalimide π···π stacking interactions of the methanol-coordinated subunit of $[Cu_4(L_{asn})_8(py)(MeOH)]$, viewed from the α face of the central subunit and the β faces of the peripheral subunits. All four rings participate in π···π stacking interactions with neighboring subunits, shown in dark (G···H "inner" interactions) and light (E···F "outer" interactions) purple.

between arms E and F, while two more form interactions on the inside of the pocket between arms G and H. The latter interactions are the stronger of the two. The vertical separations are shorter (G···H = 3.41 Å, E···F = 3.71 Å). The χ values are lower (G···H = 1.42 Å, E···F = 2.39 Å), and the naphthalimide rings are closer to coplanar (interplanar angles for G···H = 5°; for E···F = 16°). The naphthalimide−naphthalimide dipole angles for the G···H interactions are 100°, and 133° for the E···F interactions. Figure 16 shows these interactions where the central dimeric subunit is interacting with all four neighboring similar subunits (shades of purple) via π···π stacking interactions.

The structure is further supported by two of the amide arms participating in intermolecular hydrogen bonds between arm C on one pyridine coordinated subunit and arms G and F on an adjacent methanol coordinated subunit, as shown in Figure 17, which join neighboring tetramers in a one-dimensional chain that runs perpendicularly to the π-stacking interaction of the pyridine-coordinated dimeric subunit. One diethyl ether and two methanol molecules are also held into the framework by

hydrogen bonding; the ether (green) and one methanol (light orange) are hydrogen-bonded to the remaining free arm amide hydrogen atoms, while the other methanol (red) is hydrogen-bonded to the axial-coordinated methanol (yellow) of the MeOH-coordinated (purple) unit.

In the overall supramolecular structure, each tetramer π-stacks with six other tetramers and forms hydrogen bonds with two additional tetramers. Taken together, these noncovalent interactions organize the tetramers into a three-dimensional network, held together by the naphthalimide $\pi\cdots\pi$ stacking interactions supported by amide−amide hydrogen bonding. Figure 18 shows a simplified representation of this network, a drawing that shows that the structure has large pores.

The ether and one of the methanol molecules shown in Figure 17 are located in the pores formed by the surface of the tetrameric units. These pores also contain additional solvent—in addition to the ether and the methanol that hydrogen-bond to the arms of the dimers, there are three fully ordered dichloromethane molecules and a region containing disordered solvent, which refined to a mixture of dichloromethane, ether, and methanol. Figure 19 illustrates the pore, where the disordered solvent has been removed (the "empty" space). An axial view of a pore can be seen on the left (this view matches the pore seen in the center of Figure 18); the molecular surface of the tetramers is shown and the dichloromethane (yellow), ether (green), and methanol (red) molecules that occupy it. A cutaway view of the same pore is shown on the right. The disordered solvent volume occupies a total of 3973.1 Å^3 (23.2% of the unit cell volume), and the pore measures approximately 8.5 × 7.5 Å.

Single-Crystal to Single-Crystal Transformations. *[Cu$_4$($\mathbf{L_{asn}}$)$_8$(py)(S-EtLac)] (**6**).* When crystals of [Cu$_4$($\mathbf{L_{asn}}$)$_8$(py)(MeOH)] are exposed to (*S*)-ethyl lactate (CH$_3$C(H)(OH)C(O)OEt) vapor, the coordinated methanol molecule and the methanol hydrogen-bonded to it as well as the ordered solvent in the pores are replaced by (*S*)-ethyl lactate (*S*-EtLac), yielding [Cu$_4$($\mathbf{L_{asn}}$)$_8$(py)(*S*-EtLac)] (**6**) *without a loss of crystallinity*. The overall structure is closely similar to that observed for [Cu$_4$($\mathbf{L_{asn}}$)$_8$(py)(MeOH)]; one tetrameric unit is shown in Figure 20. The copper ion located at the α face of the purple subunit now is coordinated to the ester carbonyl oxygen of ethyl lactate

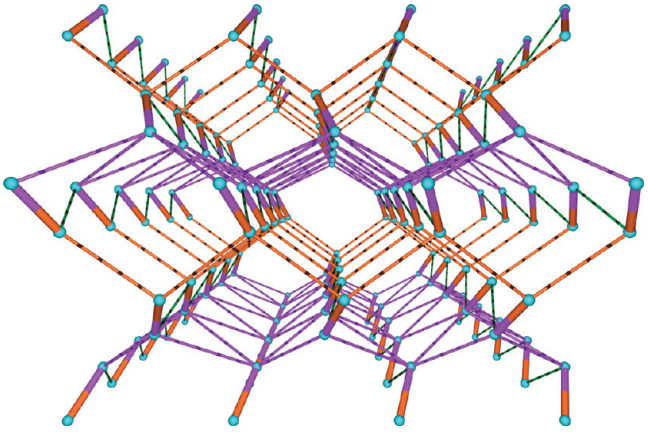

Figure 18. Simplified representation of the overall structure in [Cu$_4$($\mathbf{L_{asn}}$)$_8$(py)(MeOH)]. Individual dimeric subunits are represented by single blue spheres and the dimer−dimer covalent interaction by thick bicolored cylinders (orange = pyridine-coordinated, purple = MeOH-coordinated). The $\pi\cdots\pi$ stacking interactions (four from each purple and two from each orange subunit) are represented by thin orange and purple dashed cylinders. Intramolecular hydrogen bonds are shown as thin green dashed cylinders.

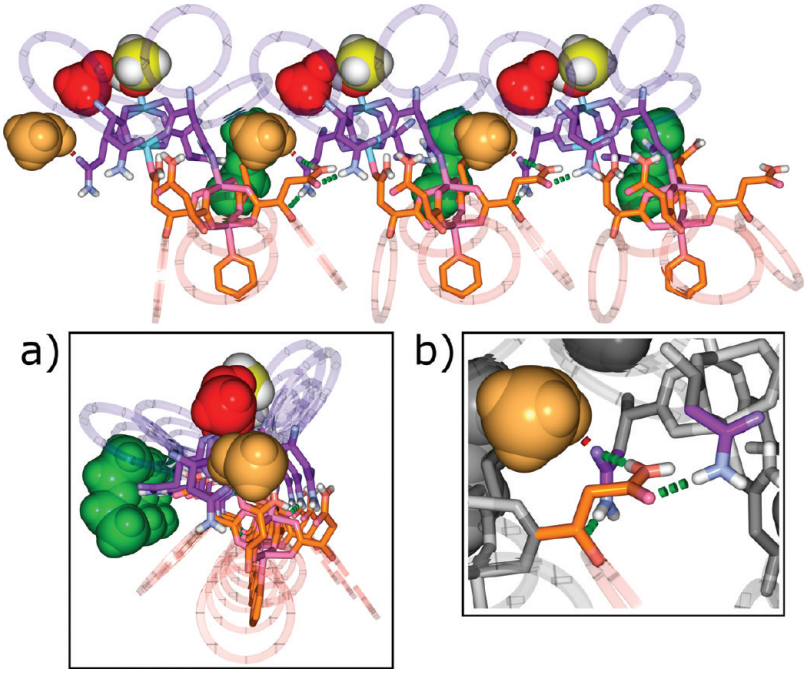

Figure 17. Chain of three hydrogen-bonded tetrameric units (top) in [Cu$_4$($\mathbf{L_{asn}}$)$_8$(py)(MeOH)]. Hydrogen bonds shown as green and red dots. The methanol-coordinated dimeric subunit (coordinated methanol as yellow space filling model) is shown in purple and the pyridine-coordinated subunit in orange. The methanol molecule hydrogen-bonded to the coordinated methanol is colored red and the ether and additional methanol molecules green and light orange, respectively, are shown as space filling models. Naphthalimide groups are shown as transparent hoops. Inset a: view of the same chain rotated by 90°. Inset b: expansion of hydrogen bonding region.

dx.doi.org/10.1021/ic201238n |*Inorg. Chem.* 2011, 50, 10225–10240

(shown in yellow and red). This axial ligand exchange changes the dimensions of the chiral pocket, which now measures 16.0 Å by 15.2 Å, a decrease of 0.5 Å in each dimension from [Cu_4($\mathbf{L_{asn}}$)$_8$(py)(MeOH)]. The chiral pocket of the pyridine-coordinated dimer is not affected by the exchange.

The pyridine-coordinated dimeric subunit (orange) has disorder in one arm (arm A\Z) and the pyridine ring. The Z disorder in arm A occurs at the CH_2-CONH_2 portion of the amide—this fragment is disordered equally over two positions. One of the disordered positions is analogous to the position of the arm A amide in [Cu_4($\mathbf{L_{asn}}$)$_8$(py)(MeOH)], and the other (referred to as amide Z) has the amide NH_2 group hydrogen-bonding with the coordinated carboxylate from arm H and the naphthalimide carbonyl oxygen of arm B. In both cases, the amide carbonyl oxygen is still coordinated with the copper ion located on the β face of the other dimeric subunit. Though the values of the intramolecular hydrogen bonds have changed, the overall connectivity of arms A−G is the same; these values and the new values for arm Z are given in Table 2.

The overall supramolecular structure of **6** is the same as that discussed above for **5**; it is dominated by each tetramer π-stacking with six other tetramers and forming hydrogen bonds with two additional tetramers. Overall, the $\pi\cdots\pi$ stacking is the same, but the metric parameters have changed somewhat, Table 3. Though some of the changes could be considered significant (>0.1 Å), none fall outside of the range for a strong naphthalimide π-stacking interaction.

Two of the amide arms participate in intermolecular hydrogen bonds that join the tetrameric units into a chain, analogous to those shown in Figure 17, inset b. The remaining free arm amide hydrogen atoms form hydrogen bonds with two additional molecules of (*S*)-ethyl lactate, one of which in turn hydrogen bonds to a third (*S*)-ethyl lactate. These interactions are illustrated in Figure 21.

The three ordered noncoordinated (*S*)-ethyl lactate molecules shown in Figure 21 are located in the pores formed by the surface of the tetrameric units. These ethyl lactates occupy the same region of the pore as the ordered solvents in [Cu_4($\mathbf{L_{asn}}$)$_8$(py)(MeOH)]. Figure 22 illustrates the pore formed by the molecular surface of the tetramers and the ethyl lactate contained within (green spacefilling models); the disordered solvent has been removed by SQUEEZE[22] (the "empty" space). An axial view of a pore is shown on the left, and a cutaway view of the same pore is shown on the right. The disordered solvent volume occupies a total of 3232.5 Å^3, or 19% of the total unit cell volume.

[Cu_4($\mathbf{L_{asn}}$)$_8$(py){(R-EtLac)$_{0.58}$(MeOH)$_{0.42}$}] (**7**). When crystals of [Cu_4($\mathbf{L_{asn}}$)$_8$(py)(MeOH)] are exposed to vapors of (*R*)-ethyl lactate for the same 48 h period as in the (*S*)-ethyl lactate experiment, again a change occurs *without a loss of crystallinity*, but in this case, the (*R*)-ethyl lactate coordinates via the −OH group, *rather than through the carbonyl oxygen.* After 48 h of exposure, the ethyl lactate has only partially displaced the axial methanol ligand; a 58/42 disordered mixture of (*R*)-ethyl lactate and methanol was located in the pocket (as determined by the refinement fixing the pocket occupancy to unity, this ratio does not change after seven days of exposure to (*R*)-ethyl lactate), giving [Cu_4($\mathbf{L_{asn}}$)$_8$(py){(*R*-EtLac)$_{0.58}$(MeOH)$_{0.42}$}] (**7**). As above, the overall structure of the tetramer is the same, and there is no change

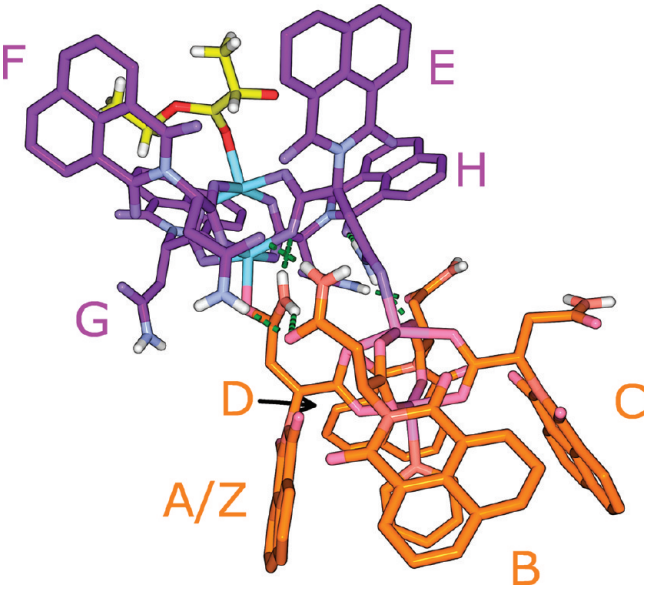

Figure 20. Drawing of one of the two disordered forms (disorder is in the A arm, only the A component is shown) of the tetramer [Cu_4($\mathbf{L_{asn}}$)$_8$(py)(*S*-EtLac)] (**6**), the form that matches the structural arrangement of [Cu_4($\mathbf{L_{asn}}$)$_8$(py)(MeOH)] shown in Figure 14. The pyridine-coordinated dimeric subunit is shown in orange and the (*S*)-ethyl lactate coordinated subunit in purple. Intramolecular hydrogen bonds are shown as green dots; hydrogen atoms attached to carbon have been omitted for clarity.

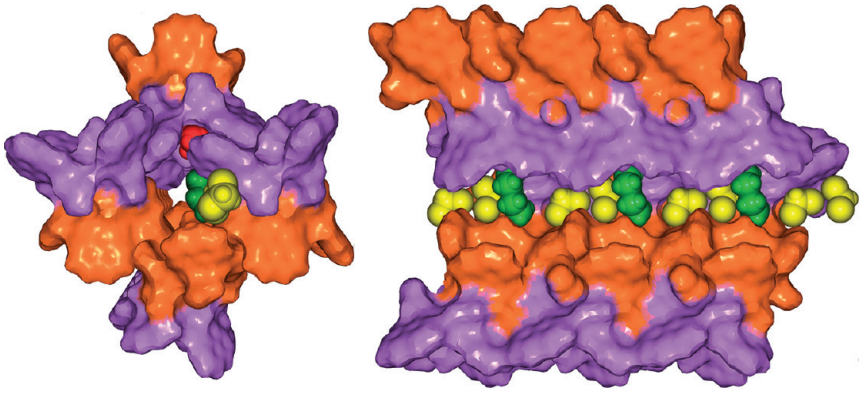

Figure 19. Two views of one pore in **5**. The molecular surface of the tetramers is shown and has been color-coded on the basis of the subunit (purple = axial ligand methanol, orange = axial ligand pyridine). The ordered solvent occupying the pores is also shown (green = ether, yellow = dichloromethane, red = methanol). Left: view down the axis of the pore; right, view from the side of the pore, with the obscuring units removed for clarity.

dx.doi.org/10.1021/ic201238n |*Inorg. Chem.* 2011, 50, 10225–10240

Table 2. Hydrogen Bonding Parameters for $[Cu_4(L_{asn})_8(py)(S\text{-EtLac})]$

D−H···A	D−H (Å)	H···A (Å)	D···A (Å)	<DHA (deg)
N(2A)−H(2A1)···O(5E)	0.88	2.37	3.07	137.4
N(2A)−H(2A2)···O(3B)	0.88	2.44	3.25	153.3
N(2B)−H(2B1)···O(3F)	0.88	2.07	2.94	170.7
N(2F)−H(2F1)···O(3B)	0.88	1.91	2.79	176
N(2E)−H(2E1)···O(5D)	0.88	2.12	2.89	146.8
N(2E)−H(2E2)···O(1H)	0.88	2.11	2.88	145.7
N(2H)−H(2H2)···O(3D)	0.88	2.01	2.86	160.4
N(2A)−H(2A1)···O(5F)	0.88	2.59	3.17	124.1
N(2Z)−H(2Z1)···O(5H)	0.88	2.27	3.01	142.1
N(2Z)−H(2Z2)···O(1D)	0.88	2.13	2.91	147.5

in the chiral pocket of the pyridine-coordinated dimer. Unlike the (*S*)-ethyl lactate experiment, no ordered solvent could be located within the pores. Both chiral pockets are similar to those in $[Cu_4(L_{asn})_8(py)(MeOH)]$, with the pyridine-coordinated dimer measuring 15.3 by 12.5 Å, and the (*R*)-ethyl lactate-coordinated dimer measuring 16.5 by 15.3 Å.

The overall supramolecular structure of **7** is the same as discussed above for **5** and **6**; it is dominated by each tetramer π-stacking with six other tetramers and forming hydrogen bonds with two additional tetramers. Again, the $\pi\cdots\pi$ stacking is the same, but the metric parameters have changed slightly, Table 4. None of the naphthalimide π-stacking interactions fall outside of the range to be considered strong.

*$[Cu_4(\mathbf{L_{asn}})_8(py)(S\text{-EtLac})]$ (**8**).* When crystals of $[Cu_4(L_{asn})_8(py)(MeOH)]$ are exposed to vapors of *racemic* ethyl lactate, the coordinated methanol molecule is displaced without a loss of crystallinity *exclusively by (S)-ethyl lactate*, yielding a new form of the tetramer $[Cu_4(L_{asn})_8(py)(S\text{-EtLac})]$ (**8**). The overall connectivity is very similar to that of **6** (one tetramer still interacts with six other tetramers via $\pi\cdots\pi$ stacking and two others through hydrogen bonding). The major difference between the structure of **8** and the structure of **6**, obtained from the vapor diffusion of pure (*S*)-ethyl lactate, is that the solvent residing in the pores in **8** is so disordered as to be essentially featureless. This disordered solvent occupies the entire volume of the pores, measuring 5875.3 Å, or a total of 33.9% of the overall unit cell volume. The values for the naphthalimide $\pi\cdots\pi$ stacking interactions in **8** have changed somewhat compared to **6**, Table 5, and the chiral pocket now measures 16.2 Å by 15.3 Å, close to that seen in **6**.

Double Exchange Experiments. Crystals of $[Cu_4(L_{asn})_8(py)(MeOH)]$ were exposed to vapors of racemic ethyl lactate yielding $[Cu_4(L_{asn})_8(py)(S\text{-EtLac})]$ (**8**), as confirmed by X-ray crystallography, again with fully disordered solvent residing in the pores. The racemic ethyl lactate was removed from this sample tube followed by exposure of these crystals of **8** to (*S*)-ethyl lactate. X-ray crystallography again confirmed that a single-crystal to single-crystal transformation had taken place yielding a new form of $[Cu_4(L_{asn})_8(py)(S\text{-EtLac})]$ (**9**). The overall connectivity of **9** is very similar to that of **6** (one tetramer still interacts with six other tetramers via $\pi\cdots\pi$ stacking and two others through hydrogen bonding). The values for the naphthalimide $\pi\cdots\pi$ stacking interactions in **9** have changed somewhat compared to **6**, Table 6, and the chiral pocket now measures 16.0 Å by 15.5 Å, close to that seen in **6**. This form differs from that obtained by exposing $[Cu_4(L_{asn})_8(py)(MeOH)]$ to pure (*S*)-ethyl lactate or racemic ethyl lactate in that *one* noncoordinated (*S*)-ethyl lactate molecule was clearly located in the pores formed by the tetrameric units, whereas three were clearly located in the formation of **6** (direct exposure of $[Cu_4(L_{asn})_8(py)(MeOH)]$ to (*S*)-ethyl lactate) and none in the formation of **8**. We note another difference in the structure of **9** is that the arrangement the (*S*)-ethyl lactate molecule located in the pores is "trans" with respect to the carbonyl and alcohol oxygen atoms, whereas all three in the pores of **6** are "cis".

Table 3. Naphthalimide $\pi\cdots\pi$ Stacking Parameters in $[Cu_4(L_{asn})_8(py)(S\text{-EtLac})]$, as compared with $[Cu_4(L_{asn})_8(py)(MeOH)]$

rings	planes distance	Δ planes distance	χ	Δ χ	planes angle	Δ planes angle	dipole angle	Δ dipole angle
G···H	3.38	−0.03	1.70	+0.28	6	+1	98	−2
E···F	3.90	+0.19	2.29	−0.10	19	+3	134	+1
B···D	3.40	−0.11	1.71	−0.13	7	−2	123	+1

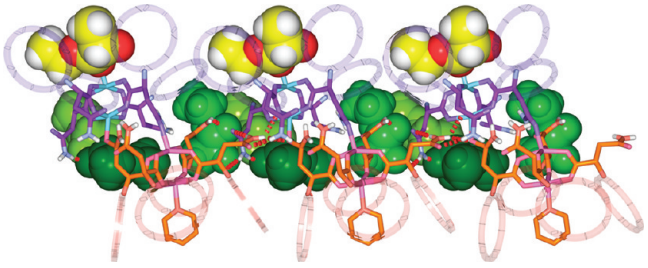

Figure 21. Chain of three hydrogen-bonded tetrameric units in $[Cu_4(L_{asn})_8(py)(S\text{-EtLac})]$ (**6**), with the hydrogen bonds shown as red dots. The ethyl lactate-coordinated dimeric subunit is shown in purple and the pyridine-coordinated subunit in orange. The metal-bonded ethyl lactate is shown as a yellow space filling model, and the three hydrogen-bonded ethyl lactate molecules are shown as green space filling models. Naphthalimide groups are shown as transparent hoops.

Crystals of $[Cu_4(L_{asn})_8(py)(MeOH)]$ were exposed to vapors of (*R*)-ethyl lactate, yielding again $[Cu_4(L_{asn})_8(py)\{(R\text{-EtLac})_{0.58}(MeOH)_{0.42}\}]$ (**7**), as confirmed by X-ray crystallography. The (*R*)-ethyl lactate was removed from this sample tube followed by exposure of these crystals (now compound **7**) to *racemic* ethyl lactate. X-ray crystallography again confirmed that a single-crystal to single-crystal transformation had taken place, yielding the same form of $[Cu_4(L_{asn})_8(py)(S\text{-EtLac})]$ (**9**) as observed in the above double exchange experiment. This experiment clearly demonstrates that the (*S*)-ethyl lactate in a racemic mixture has displaced the disordered (*R*)-ethyl lactate and MeOH in **7** and is now exclusively located in the chiral pocket.

We note that a number of other chiral substrates were briefly screened for analogous exchange properties, but to date none have been successful. Similar exchange experiments with 2-butanol, 2-butylamine, and 1-phenylethylamine all cause the crystals of $[Cu_4(L_{asn})_8(py)(MeOH)]$ to dissolve. An exchange experiment with N,N-dimethyl-1-phenylethylamine caused the crystals to change color, but the crystals were of poor quality for X-ray analysis.

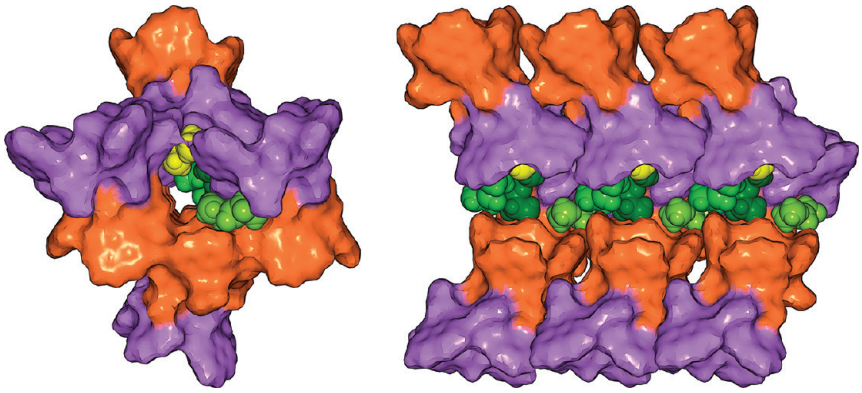

Figure 22. Two views of one pore in $[Cu_4(\mathbf{L_{asn}})_8(py)(S\text{-EtLac})]$ (**6**). The molecular surface of the tetramer is shown and has been color-coded on the basis of the subunit (purple = axial ligand ethyl lactate, orange = axial ligand pyridine). The (*S*)-ethyl lactate coordinated to the copper ion is shown in yellow, and the three ordered (*S*)-ethyl lactates occupying the pores are shown in green. Left: view down the axis of the pore; right, view from the side of the pore, with the obscuring units removed for clarity.

Table 4. Naphthalimide $\pi\cdots\pi$ Stacking Parameters in $[Cu_4(L_{asn})_8(py)(R\text{-EtLac})]$ (7), As Compared with Those in 6

rings	planes distance	Δ planes distance	χ	$\Delta\chi$	planes angle	Δ planes angle	dipole angle	Δ dipole angle
G···H	3.43	+0.05	1.63	−0.07	11	+5	101	+3
E···F	3.70	−0.20	2.54	+0.25	19	+0	138	+4
B···D	3.43	+0.03	1.49	−0.22	1	−6	123	+0

Table 5. Naphthalimide $\pi\cdots\pi$ Stacking Parameters in $[Cu_4(L_{asn})_8(py)(S\text{-EtLac})]$ (8) Compared to Those in 6

rings	planes distance	Δ planes distance	χ	$\Delta\chi$	planes angle	Δ planes angle	dipole angle	Δ dipole angle
G···H	3.44	+0.06	1.61	−0.09	6	+0	100	+2
E···F	3.70	−0.20	2.43	+0.14	20	+1	138	+4
B···D	3.46	+0.06	1.48	−0.23	2	−5	121	−2

DISCUSSION

While a main intent of the research described here was to determine the properties of copper(II) carboxylate dimers built from enantiopure carboxylate ligands containing the strong $\pi\cdots\pi$ stacking 1,8-naphthalimide synthon, the structures reported here clearly also relate to research in asymmetric rhodium dimer catalysis. The use of rhodium dimers formed from enantiopure phthalimide and naphthalimide-substituted carboxylate ligands as a catalyst in enantioselective cyclopropanation[16] and C−H insertion reactions[15] has been extensive, but only one catalyst had been structurally characterized until a recent series of publications was published. Two similar structures (crystallized from different solvents) have been carried out where the substituents on the chiral carbon are phthalimide and the relatively small benzyl group; both have the adjacent two up, two down structure shown in Figure 1a.[16a,18a] In all other published structures, the side chain is bulky, either *tert*-butyl or *iso*-propyl, and generally phthalimide is the other group at the chiral carbon. All of these structures that have the smaller phthalimide substituent (one of which is a dicopper compound[18a]) have the chiral crown configuration (twisted in one case[18a]), Figure 1d, with all of the groups on the same side of the metal dimer.[16a,17b,18a] In addition, two dirhodium compounds where the ligand contains naphthalimide and *tert*-butyl substituents have this chiral crown structure.[18]

Essentially, in all of the dicopper complexes reported here, the chiral crown configuration is observed, despite that fact that the side chain on the chiral carbon is small. In contrast to the two rhodium structures with phthalimide and the small benzyl group substituents at the chiral carbon, in the results reported here with the bulky naphthalimide group bonded to the chiral carbon, the *chiral crown* configuration is observed, even in cases where the side chain, the substituent on the other face of the dimers, is not bulky, including in three cases (complexes **1**−**3**) where this group is methyl. The partial exception to this observation is the arrangement in the structure of the EFG(H/I) dimer from $[Cu_2(\mathbf{L_{phg}})_4(THF)_2]$, where one naphthalimide group is oriented toward the β face (Figure 1c) 25% of the time. Given that the naphthalimide group appears to favor the chiral crown configuration and that in asymmetric synthesis the chiral pocket is certainly the key to selectivity, the use of the naphthalimide group in enantiopure ligands is particularly attractive for the development of catalysts, a result already observed in some,[23b,e] but not all,[23d] catalytic studies. A very recent publication has highlighted the use of the naphthalimide group in important enantioselective reactions catalyzed by rhodium dimers.[16i]

The shape of the chiral pocket is also of interest, with the asymmetry noticed in previous studies being indicated as important to the catalytic selectivity.[16g] In the structures reported here, the size and symmetry of the chiral pocket varies greatly. In $[Cu_2(\mathbf{L_{ala}})_4(THF)_2]$ and in the two forms of $[Cu_2(\mathbf{L_{phg}})_4(THF)_2]$, where a relatively small THF group is bonded to the copper ions, the pocket is nearly symmetric and relatively small, averaging 13.6 Å across the pocket with a difference in the two values for each complex not greater than 0.3 Å. The pocket is larger and more asymmetric for $[Cu_2(\mathbf{L_{ala}})_4(H\mathbf{L_{ala}})]$ and the pockets in the tetramers that do not coordinate pyridine as the axial ligand. The size of these pockets is likely influenced by the axial ligand, which varies from $H\mathbf{L_{ala}}$, methanol, and ethyl lactate. The importance of the axial ligand in the chiral pocket is more clearly indicated by the six cases where it is pyridine. In these cases, the pocket is very asymmetric due to the C−H···π interaction from the pyridine 2- and 6-position hydrogen atoms that draw in the naphthalimide groups involved in the interaction

dx.doi.org/10.1021/ic201238n |*Inorg. Chem.* 2011, 50, 10225–10240

Table 6. Naphthalimide $\pi\cdots\pi$ Stacking Parameters in $[Cu_4(L_{asn})_8(py)(S\text{-EtLac})]$ (9) Compared to Those in 6

rings	planes distance	Δ planes distance	χ	$\Delta\chi$	planes angle	Δ planes angle	dipole angle	Δ dipole angle
G···H	3.45	+0.07	1.57	−0.13	9	+3	104	+6
E···F	3.62	−0.28	2.78	+0.49	18	+1	140	+6
B···D	3.46	+0.06	1.35	−0.36	1	+6	123	+0

to an average distance of 12.0 Å, while the other two rings are separated by an average of 15.5 Å. This impact of the axial ligand may be a model for substrate interactions in the catalytic processes, as has been suggested by others.[16−18,23b]

At least in the solid state, the arrangement of the $\pi\cdots\pi$ stacking of the 1,8-naphthalimide groups, especially whether the interaction is on the inside or outside of the pocket, also impacts the size of the chiral pocket. Of course, it could be the other way around where the size of the pocket (as impacted by the axial ligand) favors one type of $\pi\cdots\pi$ stacking or the other. For example, in the asymmetric chiral pockets containing the pyridine ligands, the two well-separated naphthalimide groups not involved in the C−H$\cdots\pi$ interaction show $\pi\cdots\pi$ stacking on the inside of the pocket. Analysis of the data reported here does not support this idea that the size of the pocket strongly favors one type of $\pi\cdots\pi$ stacking where, for example, in $[Cu_2(\mathbf{L_{ala}})_4(THF)_2]$, one of the rings does an "inner" and one an "outer" $\pi\cdots\pi$ stacking interaction with its neighbors on adjacent naphthalimide groups, but the across-ring distances are short and essentially the same for both cases.

The chirality built into these complexes is manifested in these chiral pockets rather than the overall supramolecular structure. The various noncovalent interactions, mainly $\pi\cdots\pi$ stacking, that organize these solids into supramolecular structures do not result in any helical type arrangements, an arrangement we have observed with analogous enantiopure ligands that have longer connections between the 1,8-naphthalimide synthon and the amino acid.[25] In fact, many different types of supramolecular arrangements are observed in the work reported here. $[Cu_2(\mathbf{L_{ala}})_4(THF)_2]$ forms trimers that are arranged in the solid state by simple AB close packing. As can be seen in Figure 4, there are large pores in the structure, but the chiral pockets are not pointing toward these pores. $[Cu_2(\mathbf{L_{ala}})_4(H\mathbf{L_{ala}})]$ has a complex three-dimensional structure with large pores filled by solvent molecules, but both the structural arrangement and the large axial ligand isolate the chiral pocket from the pores. In contrast, $[Cu_2(\mathbf{L_{ala}})_4(py)(THF)]$ has a simple one-dimensional structure built by only two naphthalimide groups on each dimer interacting on the inside of the chiral face, and $[Cu_2(\mathbf{L_{phg}})_4(THF)_2]$ has a two-dimensional sheet structure.

The major structural change in these complexes is caused by the introduction of additional functionality, an amide group, to the side chain of the $\mathbf{L_{asn}}^-$ ligand, forming complexes where reciprocal axial coordination of one of the amide carbonyl oxygen atoms between two dimers leads to the tetramer $[Cu_4(\mathbf{L_{asn}})_8(py)(MeOH)]$ (**5**). X-ray-quality crystals were only obtained in the presence of pyridine, which acts as the axial ligand for one of the two chiral pockets of the tetramers, causing substantial asymmetry in that chiral pocket. Tetramer **5** has extensive supramolecular interactions, mainly caused by the 1,8-naphthalimide supramolecular synthon, which support an open structure containing large pores, where in this case the chiral pockets line the pores.

Given this open structure combined with the "soft" $\pi\cdots\pi$ stacking and hydrogen bonding interactions organizing the supramolecular structure,[26] it is not surprising that we have been able to observe a gas/solid-mediated single-crystal to single-crystal transformation when **5** is exposed to (*S*)-ethyl lactate *vapor*. In this transformation, the coordinated methanol molecule, the methanol molecule hydrogen-bonded to it, and the ordered (and likely disordered) solvent in the pores are replaced by (*S*)-ethyl lactate (*S*-EtLac), yielding $[Cu_4(\mathbf{L_{asn}})_8(py)(S\text{-EtLac})]$ (**6**) *without a loss of crystallinity*. There is no change in the chiral pocket containing the pyridine ligand. The low vapor pressure of ethyl lactate (2 mmHg at 20 °C) combined with a clear lack of change in the appearance of the crystals shows that this reaction is a *single-crystal to single-crystal transformation* taking place by *gas phase exchange*. These types of exchanges are rare.[27] In fact, the whole field of single-crystal to single-crystal transformations is relatively new.[27a−c,28]

Importantly, this *chiral pocket* in the tetramer is selective for coordination of (*S*)-ethyl lactate. While (*R*)-ethyl lactate vapor does cause a single-crystal to single-crystal transformation with **5**, it coordinates to the metal via the hydroxyl group rather than the ester carbonyl and does not displace all of the axially coordinated methanol ligands yielding $[Cu_4(\mathbf{L_{asn}})_8(py)\{(R\text{-EtLac})_{0.58}(MeOH)_{0.42}\}]$ (**7**). The selectivity for (*S*)-ethyl lactate is established by the exclusive formation of $[Cu_4(\mathbf{L_{asn}})_8(py)(S\text{-EtLac})]$ (**8**) in the single-crystal to single-crystal transformation of $[Cu_4(\mathbf{L_{asn}})_8(py)(MeOH)]$ with *racemic* ethyl lactate vapor. Confirmation of this selectivity is demonstrated by the *double* single-crystal to single-crystal experiment where **5** is converted to **7** in the presence of (*R*)-ethyl lactate followed by the exposure of **7** to *racemic* ethyl lactate vapor that results in the formation of $[Cu_4(\mathbf{L_{asn}})_8(py)(S\text{-EtLac})]$ (**9**). Although the tetrameric units in the structures of **8** and **9** have the same composition and very similar unit cell parameters as with **6** and each other, the overall structures are different in the ordering of the ethyl lactate in the pores. We believe this selective exchange with racemic ethyl lactate vapor to be the first example of a single-crystal to single-crystal gas/solid transformation resulting in *enantioselective bonding to a metal center*.

The preference for the occupation of the chiral pocket by (*S*)-ethyl lactate can be seen in Figures 20 and 21 and in the space filling drawing shown in Figure 23. In Figure 23, the napthalamide groups that form the chiral pocket are shown in purple, and the two naphthalimide groups from two other tetramers that $\pi\cdots\pi$ stack on the inside of the pocket (see Figure 16) are shown in two shades of blue. The hydrogen atom bonded to the chiral center of the ethyl lactate molecule (not visible in Figure 23, but clearly indicated in Figures 20 and 21) is pointed directly between the two naphthalimide groups not involved in the interior $\pi\cdots\pi$ stacking interactions. In this arrangement, the substrate clearly fits well in the pocket. Although an analogous drawing using crystallographic data cannot be generated for the *R* isomer (it bonds differently), reversal of the stereochemistry at the chiral center, leaving the hydrogen atom in the same sterically hindered position, would force the methyl group at the chiral center that is now located on the outside of the pocket to be located on the inside of the pocket (where the OH group is located), causing steric interference. Importantly, for these *solid-state* structures, the supramolecular arrangement is very important to any discussion relating to the chiral pocket—removal of the naphthalimide groups that $\pi\cdots\pi$ stack on the inside of the pocket change the pocket considerably. How this issue would

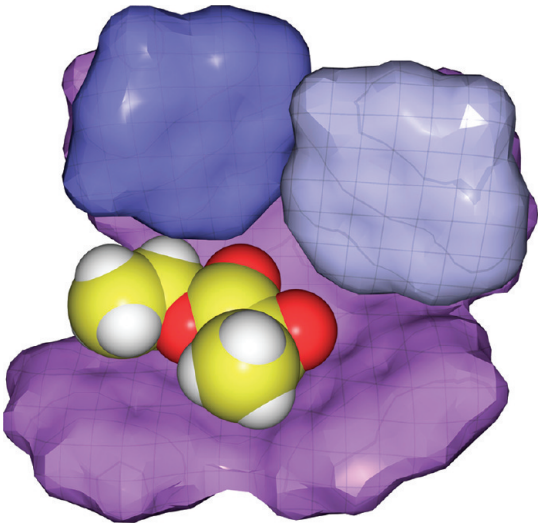

Figure 23. Space filling model of the chiral pocket of **6** showing the orientation of the (*S*)-ethyl lactate molecule. The naphthalimide groups colored in blue are from two other tetramers that $\pi\cdots\pi$ stack on the inside of the pocket of the purple-colored tetramer.

affect asymmetric *homogeneous* catalysis by these types of complexes is unclear, although we have shown in different systems that the $\pi\cdots\pi$ stacking of the naphthalimide groups can be retained in solution.[9a,c]

There is no change in space group for the single-crystal transformations reported here; the chiral pocket is large enough to bond the (*S*)-ethyl lactate without a large structural change. As can be seen in Figures 19 and 22, individual solvent or (*S*)-ethyl lactate molecules are smaller than the pores; the channels in the structures are clearly large enough to allow the exchange process of this relatively large molecule. An additional important issue is the "flexibility" imparted to these solid state structures by the $\pi\cdots\pi$ stacking interactions of the 1,8-naphthalimide supramolecular synthon. As can be seen in Tables 3−6, these interactions can change their orientations somewhat without apparently changing the strength of the interaction to any appreciable degree, allowing the structures to change slightly in these gas/solid phase exchange reactions without destroying the crystallinity. To support this idea, we have previously observed interesting single-crystal to single-crystal transformations in very different types of metal complexes whose structures are also supported by $\pi\cdots\pi$ stacking interactions of the 1,8-naphthalimide synthon.[25] In these cases, the solids have no pores to support the single-crystal to single-crystal transformations as are present in the solids reported here, but it occurs with just brief pumping or mild heating of the crystals. It appears that the naphthalimide supramolecular synthon is a functional group that has "generality" for the observation of further examples of single-crystal transformations.

CONCLUSION

The use of enantiopure ligands derived from amino acids that contain both a 1,8-naphthalimide supramolecular synthon and a carboxylate functional group for the preparation of copper(II) paddlewheel dimers has demonstrated that the chiral crown configuration of the naphthalimide groups dominates the molecular structures. The supramolecular structures are organized by $\pi\cdots\pi$ interactions of the naphthalimide groups, interactions that impact the size and shape of the chiral pocket in the solid state. Introduction of additional functionality, an amide group, to the side chain in the $\mathbf{L_{asn}}^-$ ligand leads to the formation of tetrameric $[Cu_4(\mathbf{L_{asn}})_8(py)(MeOH)]$, where reciprocal axial coordination of amide carbonyl oxygen atoms link the paddlewheel dimers. This complex has extensive supramolecular organization that forms an open structure. The structure contains one chiral pocket occupied by a pyridine ligand and another by a methanol molecule derived from the crystallization solvent. This methanol molecule exchanges enantioselectively with the (*S*)-ethyl lactate component of a racemic mixture of ethyl lactate vapor, yielding $[Cu_4(\mathbf{L_{asn}})_8(py)(S\text{-EtLac})]$ *without a loss of crystallinity*, apparently the first example of a single-crystal to single-crystal gas/solid transformation resulting in *enantioselective bonding to a metal center*.

ASSOCIATED CONTENT

Supporting Information. X-ray crystallographic files in CIF format for the structural determinations; structural refinement descriptions; tables of crystallographic information, bond distances, and bond angles; number drawings for complexes **2**−**5**; and a supramolecular structural description for compound **4**. This information is available free of charge via the Internet at http://pubs.acs.org.

AUTHOR INFORMATION

Corresponding Author
*E-mail: reger@chem.sc.edu.

ACKNOWLEDGMENT

The authors acknowledge with thanks the financial support of the U.S. National Science Foundation through grant CHE-1011736.

REFERENCES

(1) (a) Corma, A.; García, H.; Llabrés i Xamena, F. X. *Chem. Rev.* **2010**, *110*, 4606 and references therein. (b) Farrusseng, D.; Aguado, S.; Pinel, C. *Angew. Chem., Int. Ed.* **2009**, *48*, 7502. (c) Tanabe, K. K.; Cohen, S. M. *Inorg. Chem.* **2010**, *49*, 6766. (d) Lin, W. *Top. Catal.* **2010**, *53*, 869.

(2) (a) Chen, B.; Xiang, S.; Qian, G. *Acc. Chem. Res.* **2010**, *43*, 1115. (b) Liu, S.; Li, J.; Luo, F. *Inorg. Chem. Commun.* **2010**, *13*, 870. (c) Green, M. A. *Nat. Mater.* **2010**, *9*, 539. (d) Lan, A.; Li, K.; Wu, H.; Olson, D.; Emge, T.; Ki, W.; Hong, M.; Li, J. *Angew. Chem., Int. Ed.* **2009**, *48*, 2334.

(3) (a) Lee, H.; Zones, S. I.; Davis, M. E. *Nature* **2003**, *425*, 385. (b) Corma, A. *Chem. Rev.* **1997**, *97*, 2373 and references therein. (c) Czaja, A. U.; Trukhan, N.; Muller, U. *Chem. Soc. Rev.* **2009**, *38*, 1284 and references therein.

(4) Tranchemontagne, D. J.; Mendoza-Cortes, J. L.; O'Keeffe, M.; Yaghi, O. M. *Chem. Soc. Rev.* **2009**, *38*, 1257.

(5) (a) James, S. *Chem. Soc. Rev.* **2003**, *32*, 276. (b) Janiak, C. *J. Chem. Soc., Dalton Trans.* **2003**, 2781. (c) Sudik, A. C.; Cote, A. P.; Wong-Foy, A. G.; O'Keeffe, M.; Yaghi, O. M. *Angew. Chem., Int. Ed.* **2006**, *45*, 2528. (d) Stallmach, F.; Groeger, S.; Kuenzel, V.; Kaerger, J.; Yaghi, O. M.; Hesse, M.; Mueller, U. *Angew. Chem., Int. Ed.* **2006**, *45*, 2123. (e) Wong-Foy, A. G.; Matzger, Adam, J.; Yaghi, O. M. *J. Am. Chem. Soc.* **2006**, *128*, 3494. (f) Rowsell, J. C.; Yaghi, O. M. *J. Am. Chem. Soc.* **2006**, *128*, 1304. (g) Spencer, E. C.; Howard, J. K.; McIntyre, G. J.; Rowsell, J. C.; Yaghi, O. M. *Chem. Commun.* **2006**, 278. (h) Millward, A. R.; Yaghi, O. M. *J. Am. Chem. Soc.* **2005**, *127*, 17998. (i) Rowsell, J. C.; Eckert, J.;

Yaghi, O. M. *J. Am. Chem. Soc.* **2005**, *127*, 14904. (j) Ni, Z.; Yassar, A.; Antoun, T.; Yaghi, O. M. *J. Am. Chem. Soc.* **2005**, *127*, 12752. (k) Rowsell, J. C.; Spencer, E. C.; Eckert, J.; Howard, J. K.; Yaghi, O. M. *Science* **2005**, *309*, 1350. (l) Chen, B.; Ockwig, N. W.; Millward, A. R.; Contreras, D. S.; Yaghi, O. M. *Angew. Chem., Int. Ed.* **2005**, *44*, 4745. (m) Rowsell, J. L. C.; Yaghi, O. M. *Angew. Chem., Int. Ed.* **2005**, *44*, 4670. (n) Yaghi, O. M.; O'Keeffe, M.; Ockwig, N. W.; Chae, H. K.; Eddaoudi, M.; Kim, J. *Nature* **2003**, *423*, 705. (o) Eddaoudi, M.; Moler, D. B.; Li, H.; Chen, B.; Reineke, T. M.; O'Keeffe, M.; Yaghi, O. M. *Acc. Chem. Res.* **2001**, *34*, 319. (p) O'Keeffe, M.; Eddaoudi, M.; Li, H.; Reineke, T.; Yaghi, O. M. *J. Solid State Chem.* **2000**, *152*, 3. (q) Rowsell, J. L. C.; Yaghi, O. M. *Microporous Mesoporous Mater.* **2004**, *73*, 3.

(6) (a) Perry, J. J., IV; Perman, J. A.; Zaworotko, M. J. *Chem. Soc. Rev.* **2009**, *38*, 1400. (b) Moulton, B.; Zaworotko, M. J. *Curr. Opin. Solid State Mater. Sci.* **2002**, *6*, 117. (c) Moulton, B.; Zaworotko, M. J. *Chem. Rev.* **2001**, *101*, 1629.

(7) (a) Horike, S.; Shimomura, S.; Kitagawa, S. *Nat. Chem.* **2009**, *1*, 695. (b) Kitagawa, S.; Uemura, K. *Chem. Soc. Rev.* **2005**, *34*, 109.

(8) (a) Janiak, C. *J. Chem. Soc., Dalton Trans.* **2000**, 3885 and references therein. (b) Claessens, C. G.; Stoddart, J. F. *J. Phys. Org. Chem.* **1997**, *10*, 254. (c) Guo, H.; Guo, X.; Batten, S. R.; Song, J.; Song, S.; Dang, S.; Zheng, G.; Tang, J.; Zhang, H. *Cryst. Growth Des.* **2009**, *9*, 1394.

(9) (a) Reger, D. L.; Elgin, J. D.; Semeniuc, R. F.; Pellechia, P. J.; Smith, M. D. *Chem. Commun.* **2005**, 4068. (b) Reger, D. L.; Semeniuc, R. F.; Elgin, J. D.; Rassolov, V.; Smith, M. D. *Cryst. Growth Des.* **2006**, *6*, 2758. (c) Reger, D. L.; Elgin, J. D.; Smith, M. D; Simpson, B. K. *Polyhedron* **2009**, *28*, 1469.

(10) Reger, D. L.; Debreczeni, A.; Reinecke, B.; Rassolov, V.; Smith, M. D.; Semeniuc, R. F. *Inorg. Chem.* **2009**, *48*, 8911.

(11) (a) Cotton, F. A.; Wilkinson, G; Murillo, C. A.; Bochmann, M. *Adv. Inorg. Chem.*; John Wiley & Sons, Inc.: New York, 1999; 870−871. (b) Kahn, O. *Molecular Magnetism*; VCH Publishers, Inc.: New York, 1993. (c) Yougme, S.; Cheansirisomboon, A.; Danvirutai, C.; Pakawatchai, C.; Chaichit, N.; Engkagul, C.; van Albada, A. G.; Costa, J. S.; Reedijk, J. *Polyhedron* **2008**, *27*, 1875. (d) Kato, M; Muto, Y. *Coord. Chem. Rev.* **1988**, *92*, 45. (e) Melnik, M. *Coord. Chem. Rev.* **1982**, *42*, 259.

(12) Magnetism: (a) Coronado, E.; Dunbar, K. R. *Inorg. Chem.* **2009**, *48*, 3293 and references therein. (b) Train, C.; Gheorghe, R.; Krstic, V.; Chamoreau, L.-M.; Ovanesyan, N. S.; Rikken, G. L. J. A.; Gruselle, M.; Verdaguer, M. *Nat. Mater.* **2008**, *7*, 729. (c) Barron, L. D. *Nat. Mater.* **2008**, *7*, 691 and references therein.

(13) Catalysis: (a) Corma, A.; García, H.; Llabrés i Xamena, F. X. *Chem. Rev.* **2010**. *110*, 4606 and references therein. (b) Farrusseng, D.; Aguado, S.; Pinel, C. *Angew. Chem., Int. Ed.* **2009**, *48*, 7502–7513. (c) Tanabe, K. K.; Cohen, S. M. *Inorg. Chem.* **2010**, *49*, 6766. (d) Lin, W. *Top. Catal.* **2010**, *53*, 869.

(14) Sensors: (a) Chen, B.; Xiang, S.; Qian, G. *Acc. Chem. Res.* **2010**, *43*, 1115. (b) Liu, S.; Li, J.; Luo, F. *Inorg. Chem. Commun.* **2010**, *13*, 870. (c) Green, M. A. *Nat. Mater.* **2010**, *9*, 539. (d) Lan, A.; Li, K.; Wu, H.; Olson, D.; Emge, T.; Ki, W.; Hong, M.; Li, J. *Angew. Chem., Int. Ed.* **2009**, *48*, 2334. (e) Chen, B.; Wang, L.; Zapata, F.; Qian, G.; Lobkovsky, E. B. *J. Am. Chem. Soc.* **2008**, *130*, 6718. (f) Chen, B.; Wang, L.; Xiao, Y.; Fronczek, F.; Xue, M.; Cui, Y.; Qian, G. *Angew. Chem., Int. Ed.* **2009**, *48*, 500.

(15) Sieves: (a) Lee, H.; Zones, S. I.; Davis, M. E. *Nature* **2003**, *425*, 385. (b) Corma, A. *Chem. Rev.* **1997**, *97*, 2373 and references therein. (c) Czaja, A. U.; Trukhan, N.; Muller, U. *Chem. Soc. Rev.* **2009**, *38*, 1284 and references therein.

(16) (a) Hashimoto, S.; Watanabe, N.; Sato, T.; Shiro, M.; Ikegami, S. *Tetrahedron Lett.* **1993**, *34*, 5109. (b) Anada, M.; Hashimoto, S. *Tetrahedron Lett.* **1998**, *39*, 79. (c) Minami, K.; Saito, H.; Tsutsui, H.; Nambu, H.; Anada, M.; Hashimoto, S. *Adv. Synth. Catal.* **2005**, *347*, 1483. (d) Hashimoto, S.; Watanabe, N.; Ikegami, S. *Tetrahedron Lett.* **1990**, *31*, 5173. (e) Collet, F.; Dodd, R.; Dauban, P. *Org. Lett.* **2008**, *10*, 5473. (f) Davies, H. M.; Hedley, S. J.; Bohall, B. R. *J. Org. Chem.* **2005**, *70*, 10737. (g) DeAngelis, A.; Dmitrenko, O.; Yap, G. P. A.; Fox, J. M. *J. Am. Chem. Soc.* **2009**, *131*, 7230. (h) Natori, Y.; Tsutsui, H.; Sato, N.; Nakamura, S.; Nambu, H.; Shiro, M.; Hashimoto, S. *J. Org. Chem.* **2009**, *74*, 4418. (i) DeAngelis, A.; Shurtleff, V. W.; Dmitrenko, O.; Fox, J. M. *J. Am. Chem. Soc.* **2011**, *133*, 1650.

(17) (a) González-Bobes, F.; Fenster, M. D.; Kiau, S.; Kolla, L.; Kolotuchin, S.; Soumeillant, M. *Adv. Synth. Catal.* **2008**, *350*, 813. (b) Lindsay, V. N.; Lin, W.; Charette, A. B. *J. Am. Chem. Soc.* **2009**, *131*, 16383. (c) Müller, P.; Bernardinelli, G.; Allenbach, Y. F.; Ferri, M.; Flack, H. D. *Org. Lett.* **2004**, *6*, 1725. (d) Ghanem, A.; Lacrampe, F.; Schurig, V. *Helv. Chim. Acta* **2005**, *88*, 216.

(18) (a) DeAngelis, A.; Boruta, D. T.; Lubin, J.; Plampin, J. N., III; Yap, G. P. A.; Fox, J. M. *Chem. Commun.* **2010**, *46*, 4541. (b) Ghanem, A.; Gardiner, M.; Williamson, R.; Müller, P. *Chem.—Eur. J.* **2010**, *16*, 3291.

(19) Reger, D. L.; Horger, J.; Smith, M. D. *Chem. Commun.* **2011**, *47*, 2805.

(20) (a) *SMART*, version 5.630; *SAINT+*, version 6.45; *SADABS*, version 2.05; Bruker Analytical X-ray Systems, Inc.: Madison, WI, 2003.

(21) Sheldrick, G. M. *SHELXTL*, version 6.14; Bruker Analytical X-ray Systems, Inc.: Madison, WI, 2000.

(22) Spek, A. L. *Acta Crystallogr., Sect. A* **1990**, *46*, C34. (b) Spek, A. L. *PLATON*; Utrecht University: Utrecht, The Netherlands, 1998.

(23) (a) Jursic, B. S.; Patel, P. K. *Tetrahedron* **2005**, *61*, 919. (b) Liang, C.; Collet, F.; Robert-Peillard, F.; Müller, P.; Dodd, R. H.; Dauban, P. *J. Am. Chem. Soc.* **2008**, *130*, 343. (c) Collet, F.; Dodd, R. H.; Dauban, P. *Org. Lett.* **2008**, *10*, 5473. (d) Davies, H. M. L.; Hedley, S. J.; Bohall, B. R. J. *Org. Chem.* **2005**, *70*, 10737. (e) Müller, P.; Bernardinelli, G.; Allenbach, Y. F.; Ferri, M.; Flack, H. D. *Org. Lett.* **2004**, *6*, 1725.

(24) Hansen, J.; Davies, H. *Coord. Chem. Rev.* **2008**, *252*, 545.

(25) (a) Reger, D. L.; Horger, J.; Smith, M. D.; Long, G. J. *Chem. Commun.* **2009**, 6219. (b) Reger, D. L.; Horger, J. J.; Smith, M. D.; Long, G. J.; Fernande, G. *Inorg. Chem.* **2011**, *50*, 686.

(26) (a) Noro, S. *Phys. Chem. Chem. Phys.* **2010**, *12*, 2519. (b) Bersuker, I. *J. Mol. Struct.* **2007**, *838*, 44. (c) Zhang, J.; Chen, X. *J. Am. Chem. Soc.* **2009**, *131*, 5516. (d) Horike, S.; Shimomura, S.; Kitagawa, S. *Nat. Chem.* **2009**, *1*, 695. (e) Fletcher, A.; Thomas, K.; Rosseinsky, M. *J. Solid State Chem.* **2005**, *178*, 2491. (f) Bradshaw, D.; Claridge, J. B.; Cussen, E. J.; Prior, T. J.; Rosseinsky, M. J. *Acc. Chem. Res.* **2005**, *38*, 273.

(27) (a) Huang, Z.; White, P.; Brookhart, M. *Nature* **2010**, *465*, 598. (b) Xue, D.; Zhang, W.; Chen, X.; Wang, H. *Chem. Commun.* **2008**, 1551. (c) Atwood, J. L.; Barbour, L. J.; Jerga, A.; Schottel, B. L. *Science* **2002**, *298*, 1000. (d) Cotton, F. A.; Li, Z.; Murillo, C. A.; Wang, X.; Yu, R.; Zhao, Q. *Inorg. Chem.* **2007**, *46*, 3245. (e) Ghosh, S.; Zhang, J.; Kitagawa, S. *Angew. Chem., Int. Ed.* **2007**, *46*, 7965. (f) Ghosh, S.; Kaneko, W.; Kiriya, D.; Ohba, M.; Kitagawa, S. *Angew. Chem., Int. Ed.* **2008**, *47*, 8843. (g) Warren, M.; Brayshaw, S.; Johnson, A.; Schiffers, S.; Raithby, P.; Easun, T.; George, M.; Warren, J.; Teat, S. *Angew. Chem., Int. Ed.* **2009**, *48*, 5711. (h) Li, B.; Wei, R.; Tao, J.; Huang, R.; Zheng, L.; Zheng, Z. *J. Am. Chem. Soc.* **2010**, *132*, 1558.

(28) Halder, G. J.; Kepert, C. J. *Aus. J. Chem.* **2006**, *59*, 597 and references therein.